Update on the National Ignition Campaign

Siegfried H. Glenzer
Lawrence Livermore National Laboratory

NIF User Group Meeting

February 14, 2012

This work performed under the auspices of the U.S. Department of Energy by Lawrence Livermore National Laboratory under Contract DE-AC52-07NA27344

Summary

- We have successfully completed the first integrated ignition tuning experiments by fielding ~ twenty $T_{70\text{-}74}H_{20\text{-}24}D_{2\text{-}20}$ and $D_{50}T_{50}$ implosions
  - Ability to field cryogenic thermonuclear fuel layers that meet ignition specification
  - Use of varying amounts of deuterium allows for a diagnostic rich environment to measure the assembly of thermonuclear fuel

- These experiments have demonstrated high values for the Lawson fusion confinement criterion
  - Implosion are driven up to 1.6 MJ in >300 eV hohlraums
  - Demonstrated control of implosion shape
  - Demonstrated 8 x 10^{14} DT yield with 10-20% yield over 2-D clean
  - Demonstrated pressures > 100 Gbar and experimental ignition threshold factors of ITFx ~ 0.1

- Next tuning steps include
  - Shape, Entropy, Velocity, Mix

We are at the threshold of delivering a DT platform to measure α−heating

Implosions with thermonuclear fuel use DT ice layers in CH capsules that are driven in Au hohlraums with temperatures >300 eV

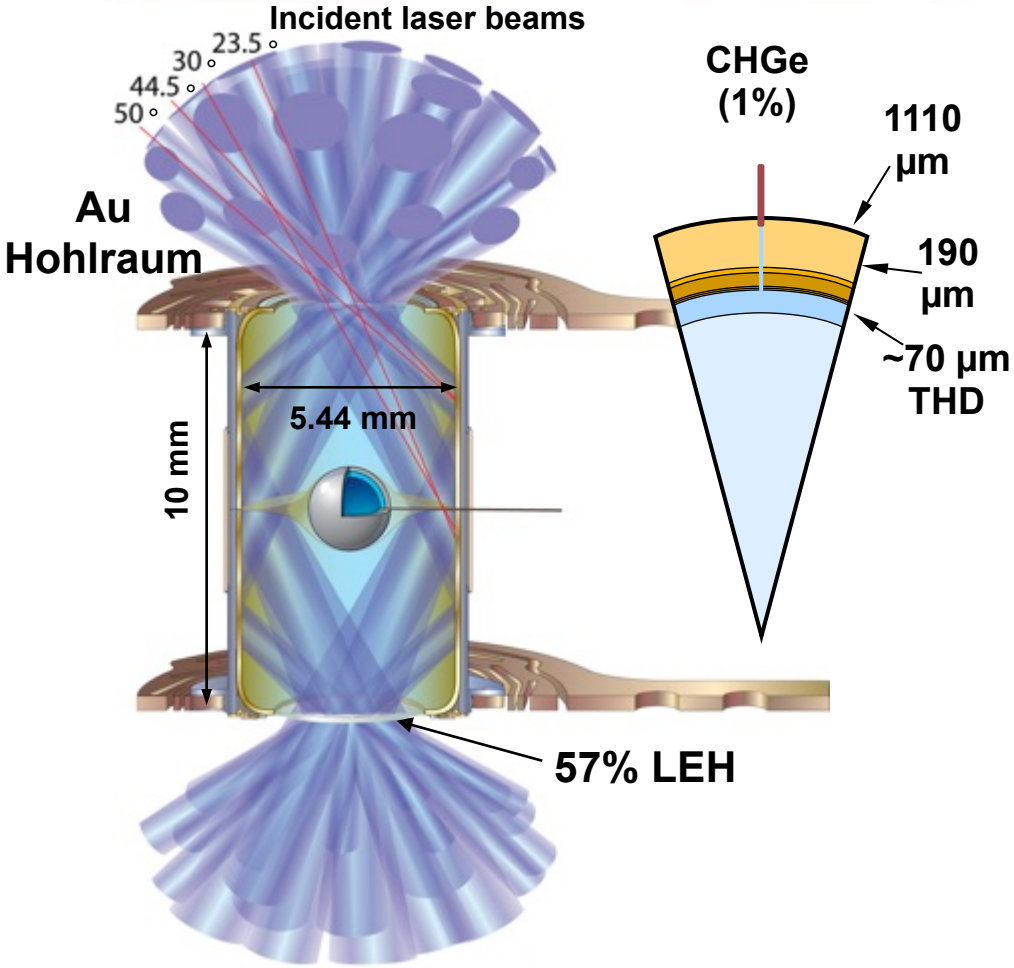

(0.96 ± 0.01) mg/cc
He gas fill

Scale 544 hohlraum with CH/Ge capsule

First layered implosions at 1 MJ laser energy in September 2010

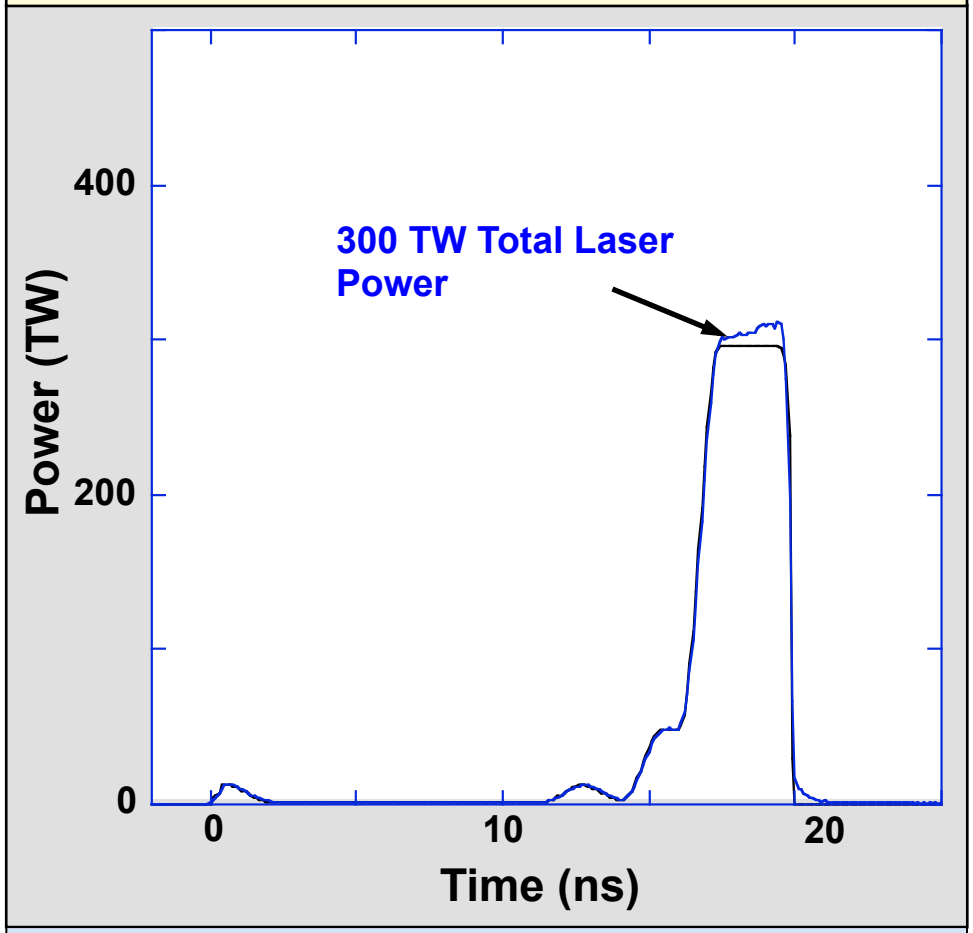

Experiment uses smoothed beams with polarization rotators, $\Delta\omega_{SSD}$ = 45 GHz, $\Delta\lambda$ = 8 Å

Implosions with thermonuclear fuel use DT ice layers in CH capsules that are driven in Au hohlraums with temperatures >300 eV

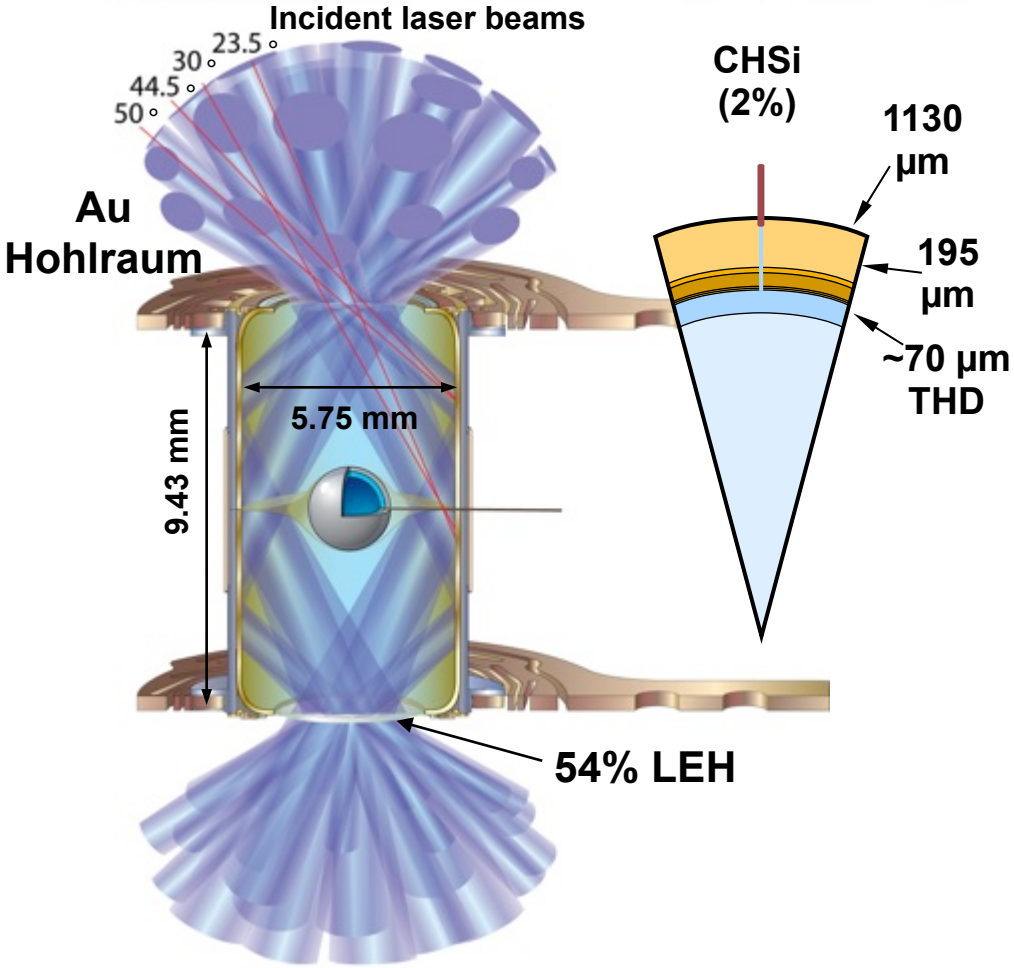

(0.96 ± 0.01) mg/cc He gas fill

Scale 575 hohlraum with CH/Si capsule

Current implosions 1.6 MJ laser energy at 430 TW reach (350 ± 20) km/s

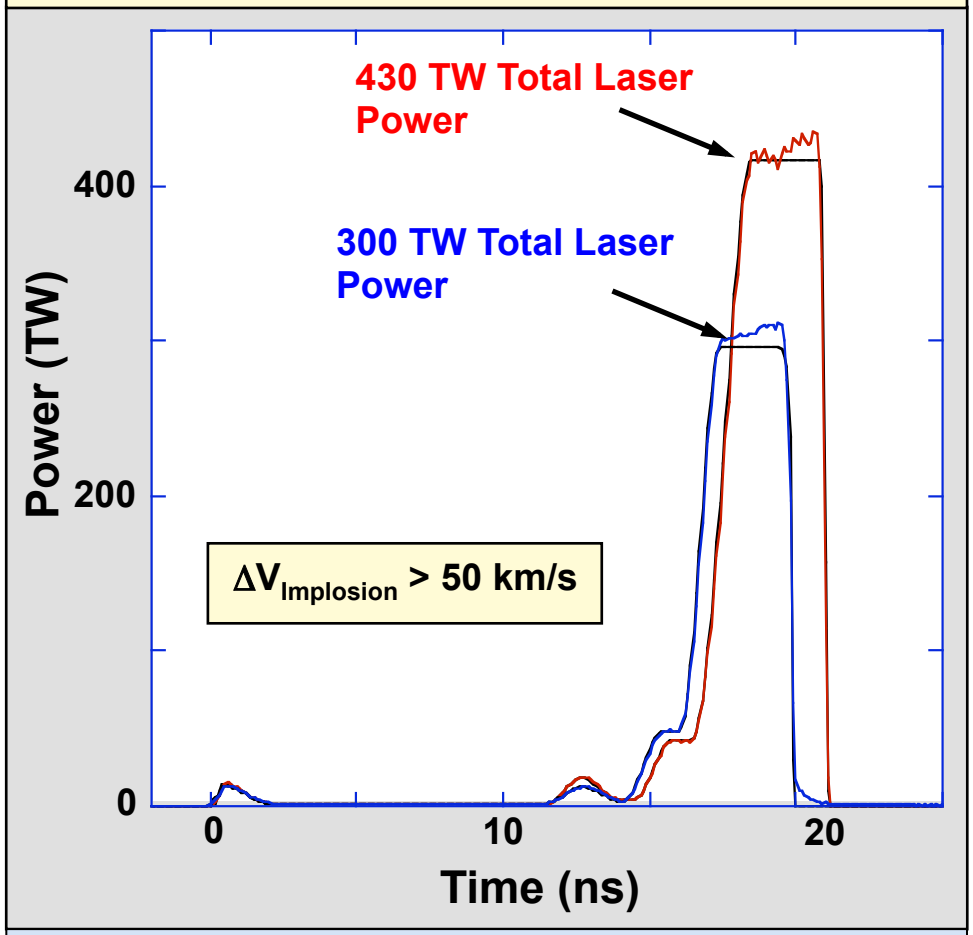

- Velocity within 5% of ignition requirement - 300 ps longer drive avoids coasting

Layered implosions are driven with fully tuned – shock-timed – laser pulses throughout the 4 shocks

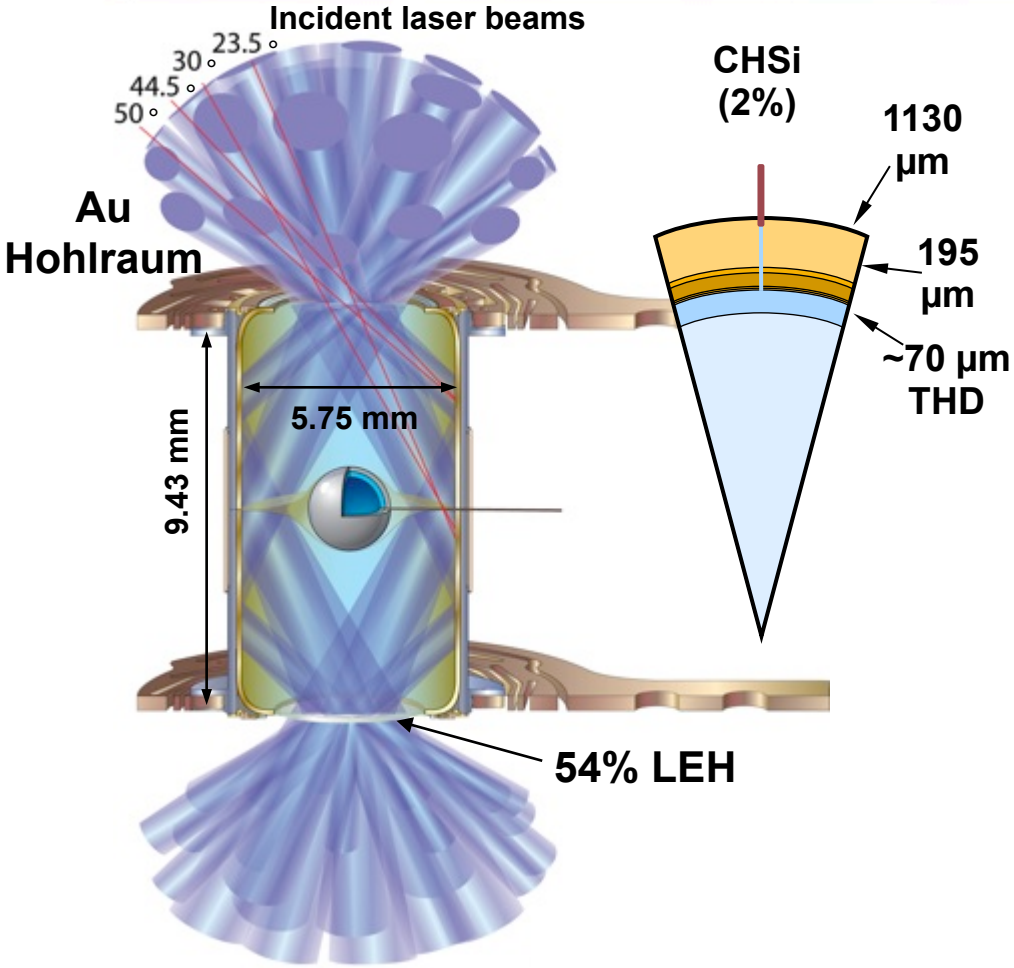

(0.96 ± 0.01) mg/cc He gas fill

Scale 575 hohlraum with CH/Si capsule

Current implosions 1.6 MJ laser energy at 430 TW reach (350 ± 20) km/s

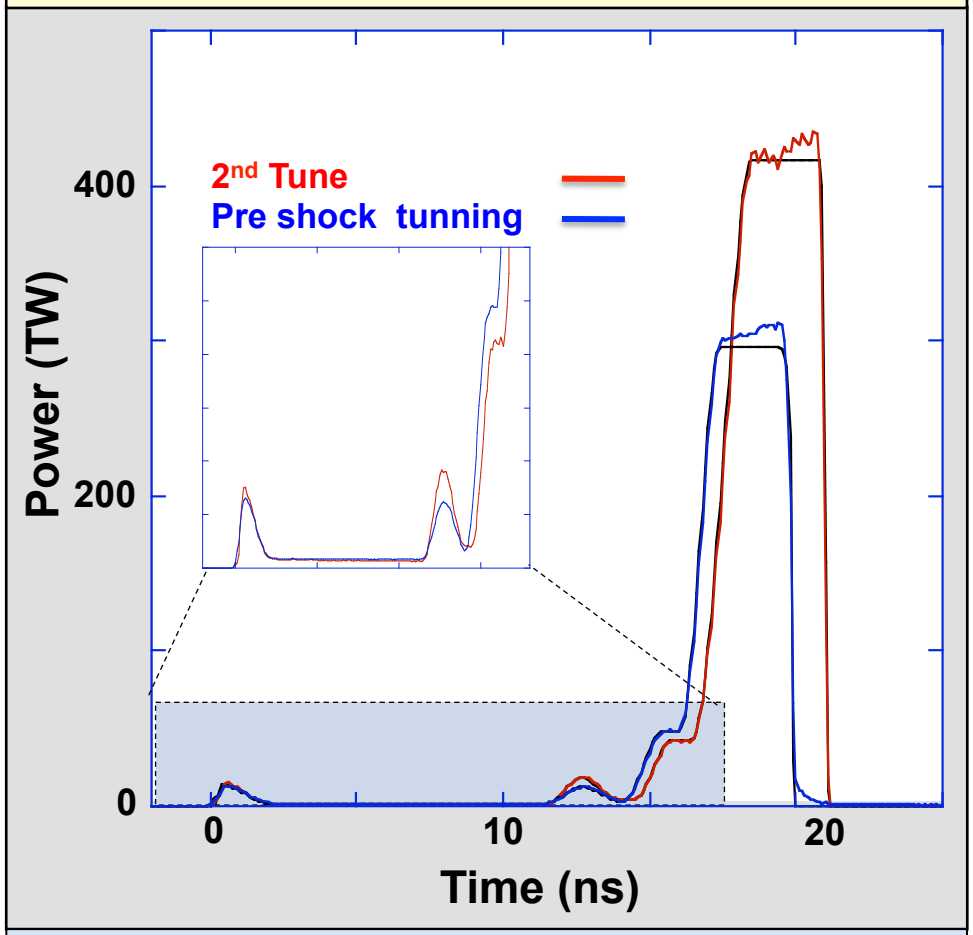

Tuned laser pulse achieved adequate shock coalescence with $\rho R = 1$ g/cm^2

Layered implosions are driven with fully tuned – i.e. symmetry tuned – laser pulses throughout the 4 shocks

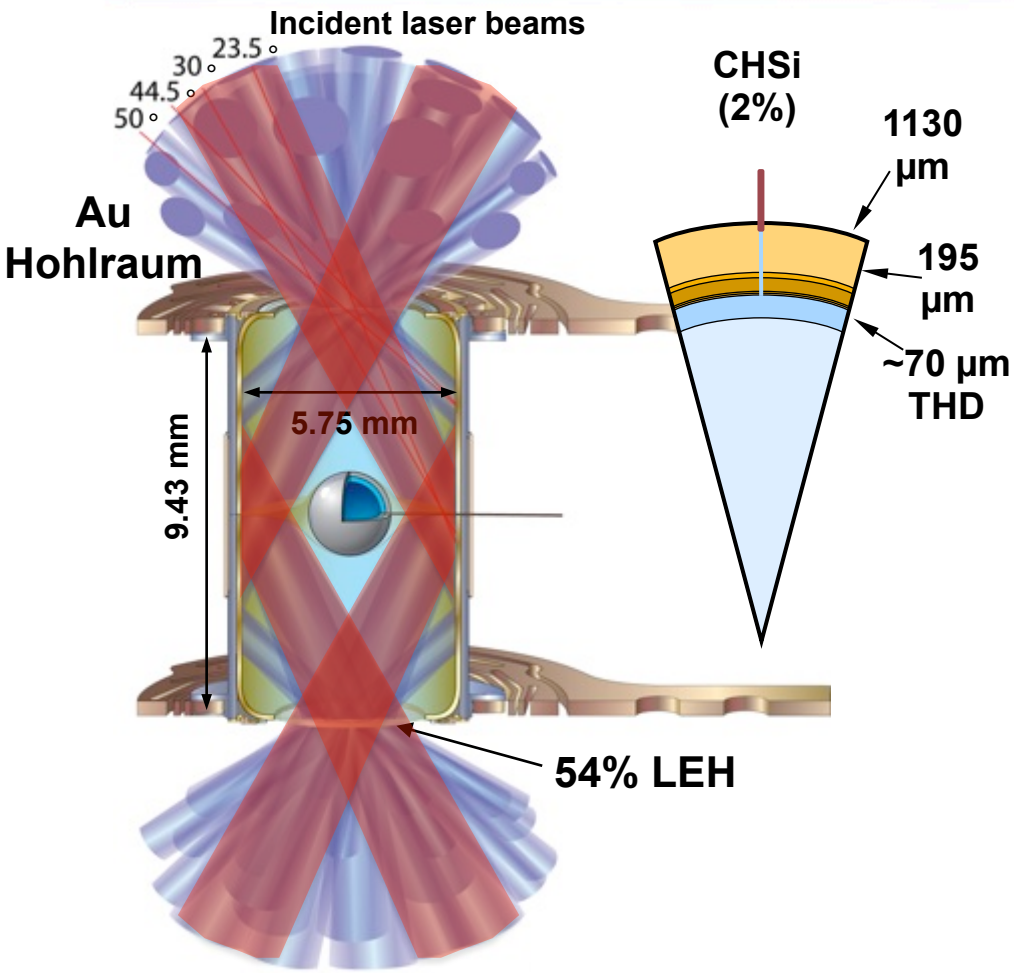

(0.96 ± 0.01) mg/cc
He gas fill

Tuned Power Cone Fraction:
P_{inner} / P_{Total}

Tuning platforms have delivered the pulse shape and power cone fraction

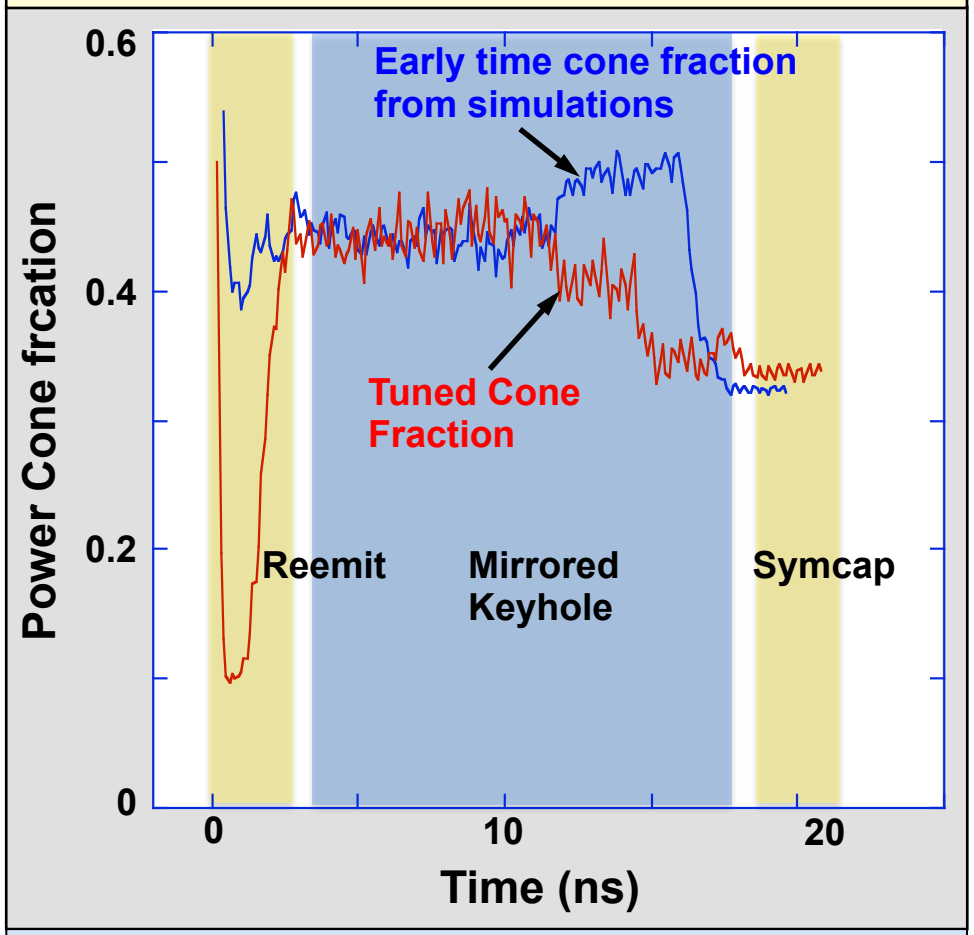

We transitioned from a ~20 shot shape tuning campaign with symmetry (t) to pressure tuning

Hard x-ray imaging indicate hohlraum laser beam coupling

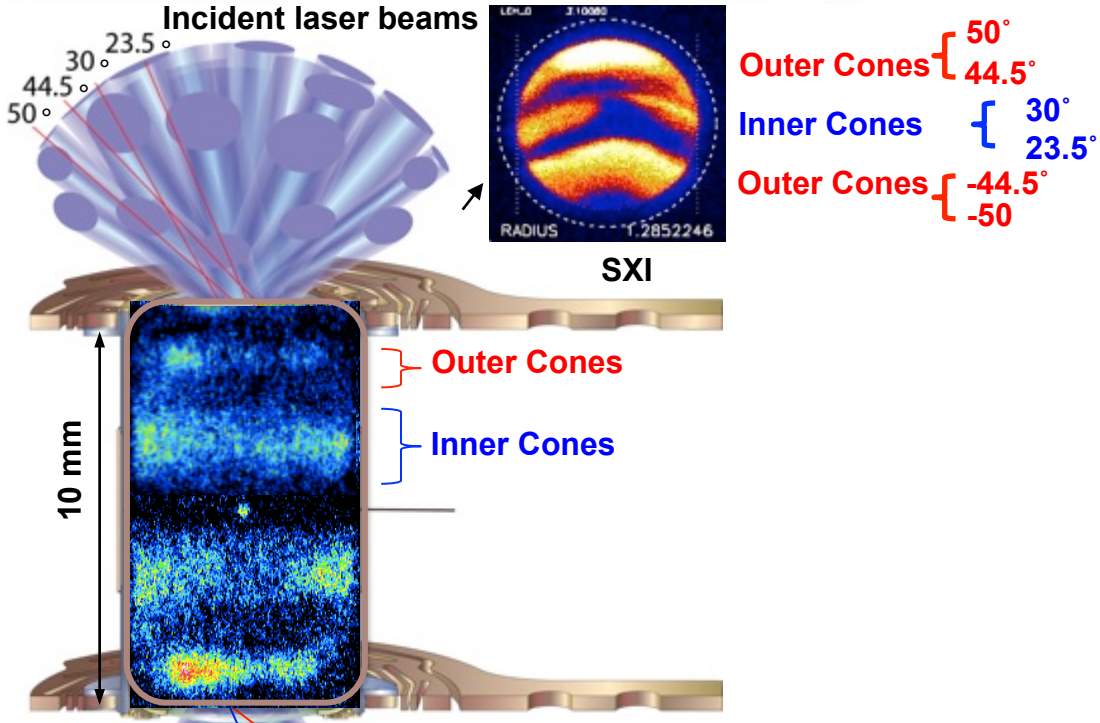

Preheat:
Hard x-ray detector
- FFLEX

Outer Cone
backscatter
- FABS & NBI Q36B

Inner Cone backscatter
- FABS & NBI Q31B

Soft x-ray drive and
preheat
- DANTE

The experiments have highly compressed 0.16 mg DT layered fuel capsules producing a 50 μm hot spot plasma

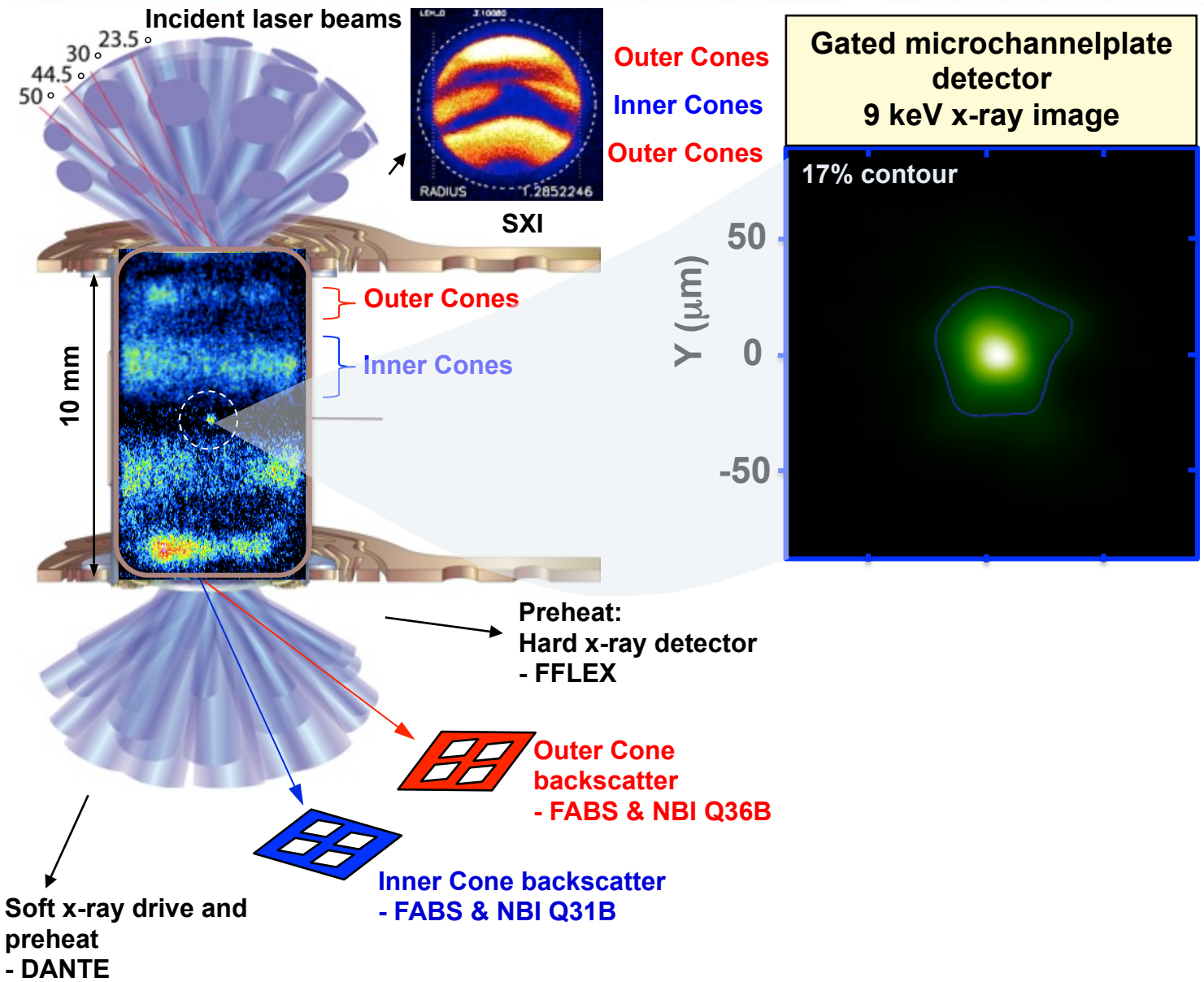

Initial capsule diameter: 2.26 mm

Emitting region 50x smaller than capsule diameter

Good symmetry at peak compression:
P_2/P_0= 3.2%
P_0 = 24 μm

The experiments have highly compressed 0.16 mg DT layered fuel capsules producing a 50 μm hot spot plasma

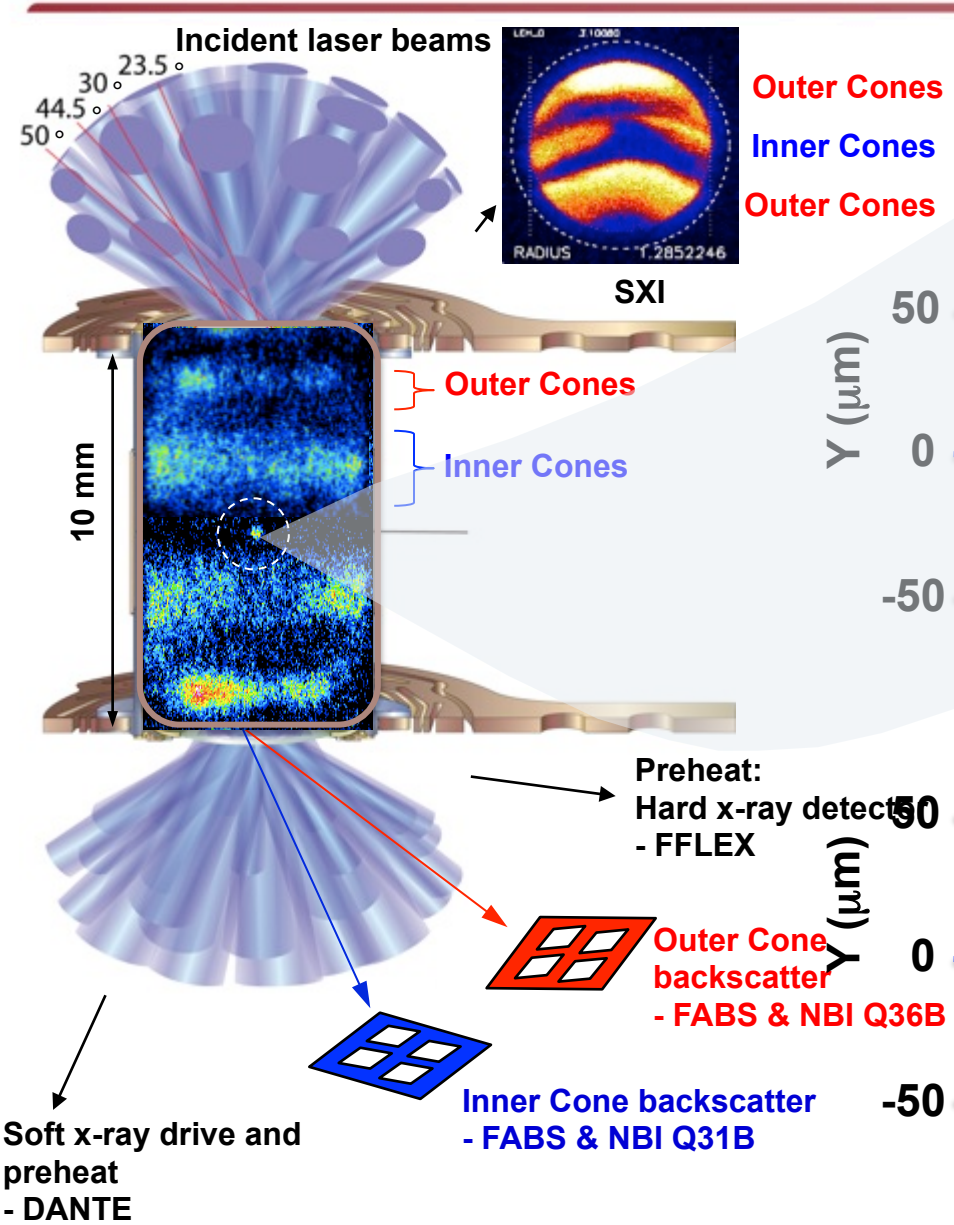

Good symmetry seen in x-ray and neutron images

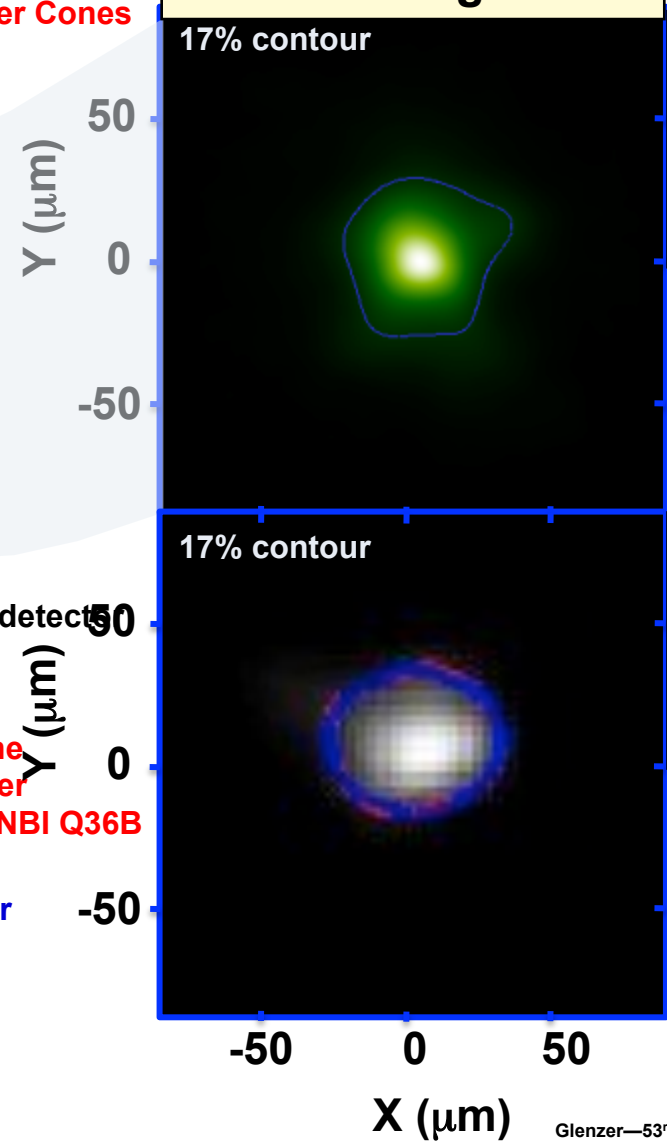

Gated microchannelplate detector
9 keV x-ray image
P_2/P_0= 3.2%
P_0 = 24 ± 2 μm

Gated 13-15 MeV neutron image
Primary neutrons
P_2/P_0= -14%
P_0 = 27 ± 4 μm

The experiments have highly compressed 0.16 mg DT layered fuel capsules producing fuel densities of 500 g/cm^3

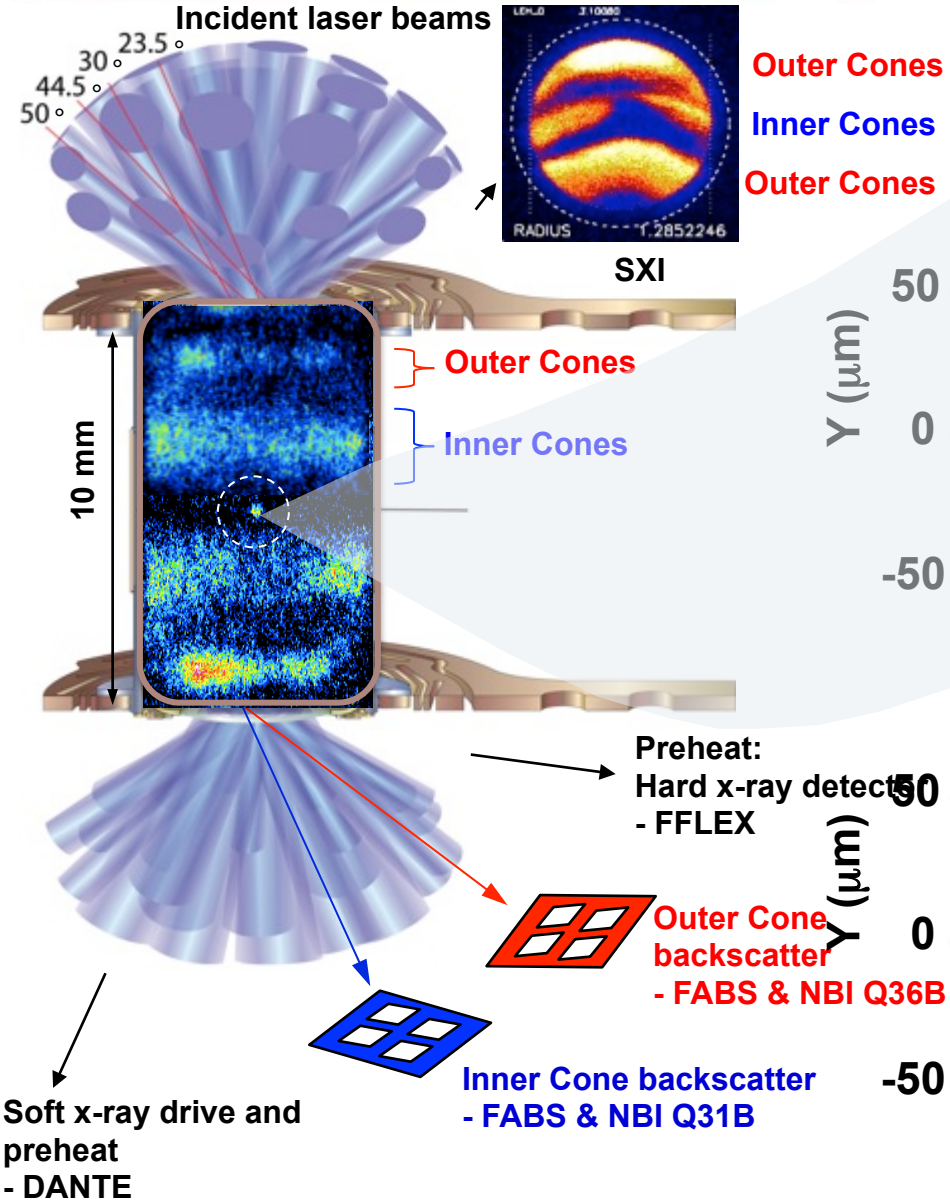

Consistent with ~25 compression; ρ >500 g/cm^3, P > 100Gbar

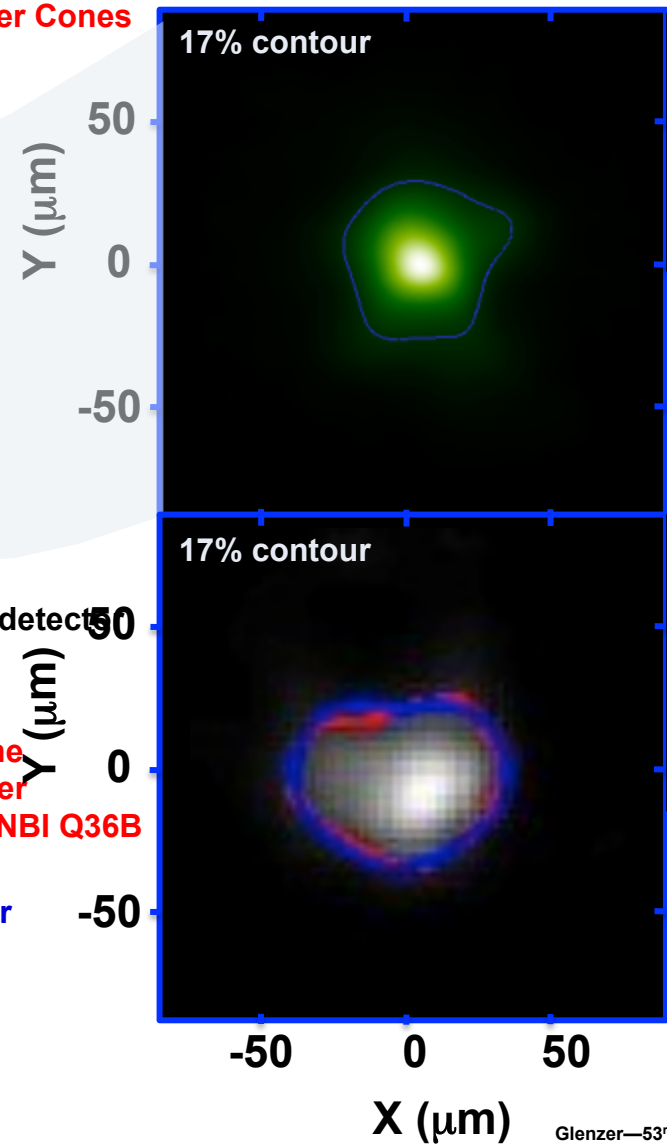

Gated microchannelplate detector
9 keV x-ray image
P_2/P_0= 3.2%
P_0 = 24 ± 2 μm

Gated 10-12 MeV neutron image
Neutrons scattered in the shell
P_2/P_0= -19%
P_0 = 35 ± 4 μm

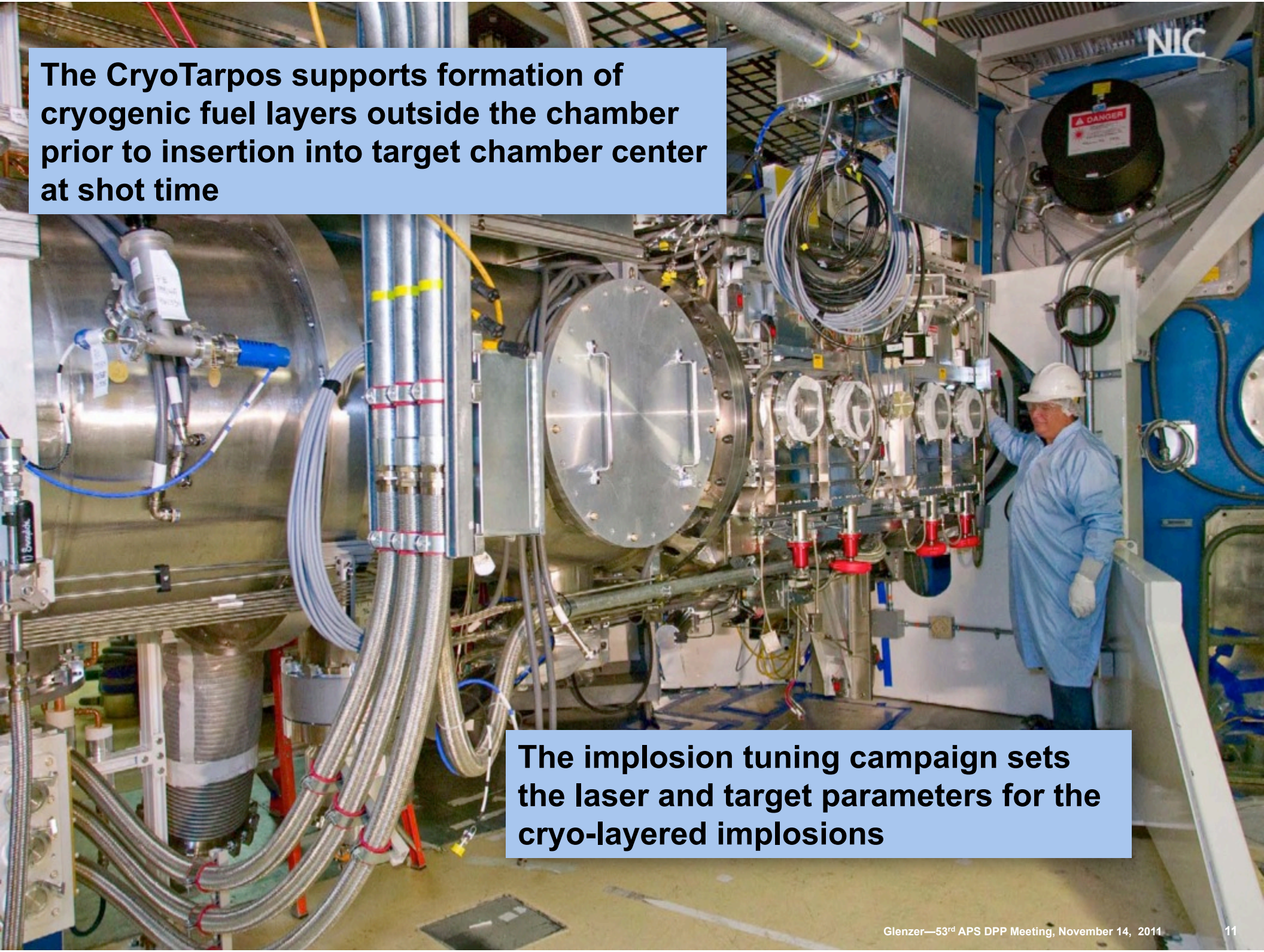

The CryoTarpos supports formation of cryogenic fuel layers outside the chamber prior to insertion into target chamber center at shot time

The implosion tuning campaign sets the laser and target parameters for the cryo-layered implosions

Inserting the target on the tip of the target positioner
Cryo-shroud retracted

THD fuel layers are formed with the target mounted in a dedicated cryogenic target positioner thermally isolated by a removable shroud

27850001 target in layering shroud

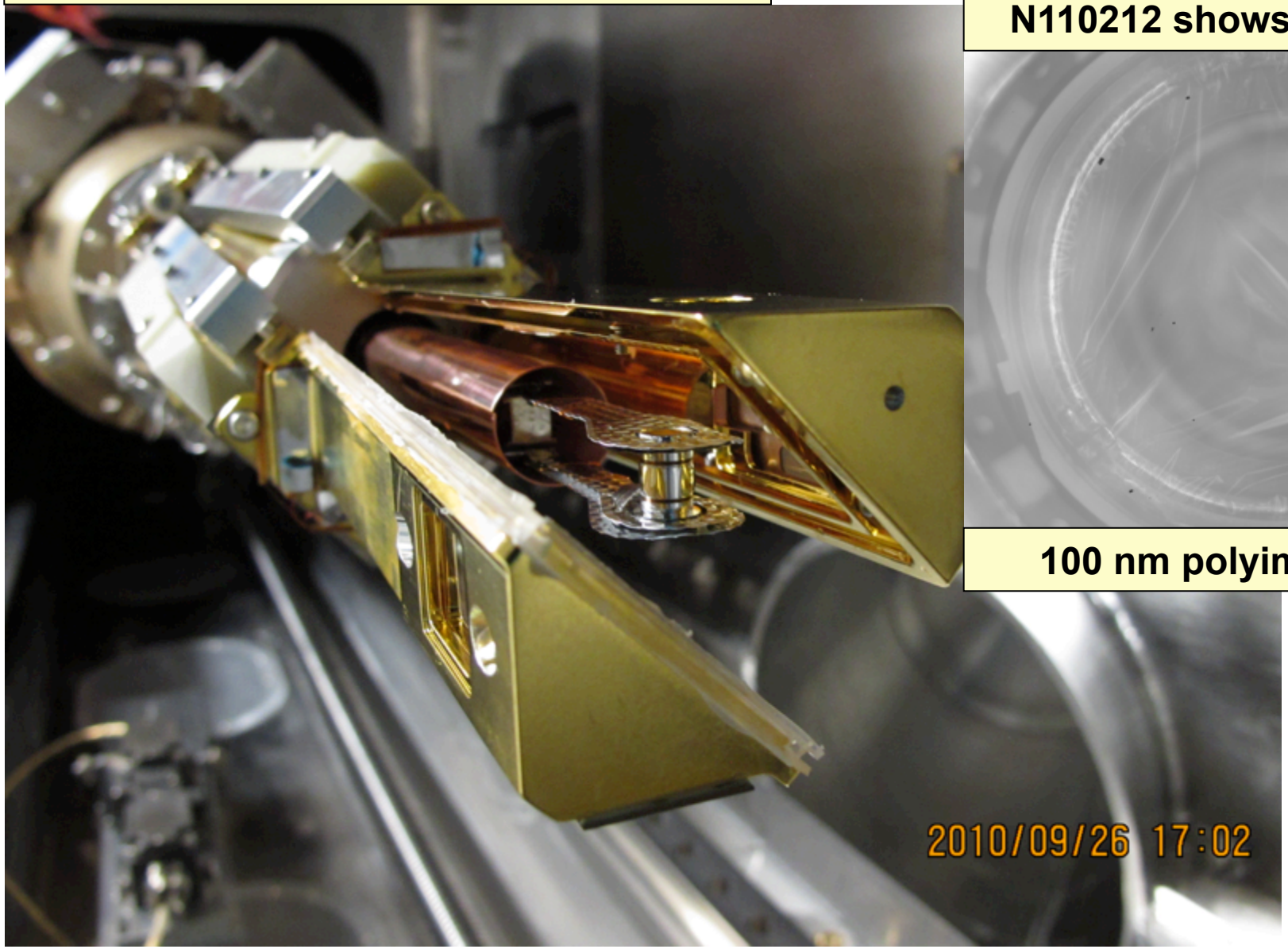

Alignment camera for shot N110212 shows storm window

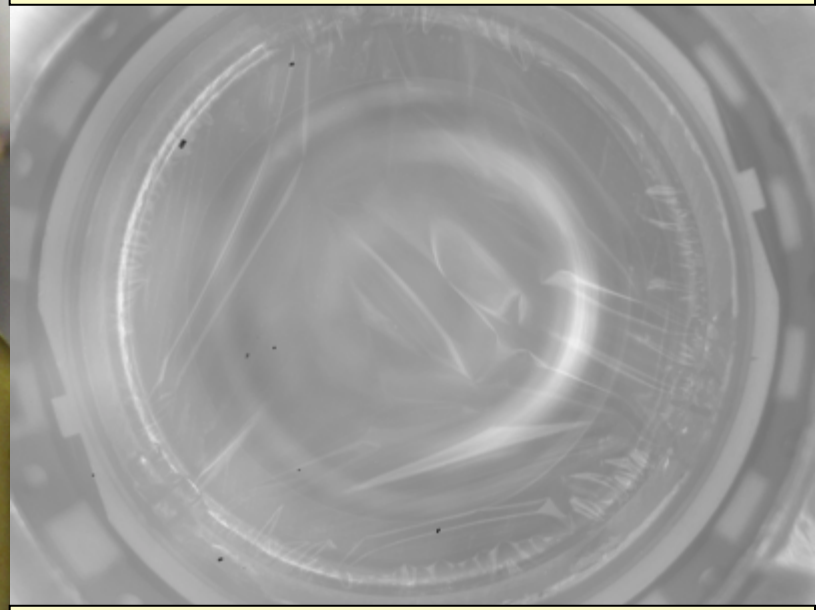

100 nm polyimide, 40 nm C

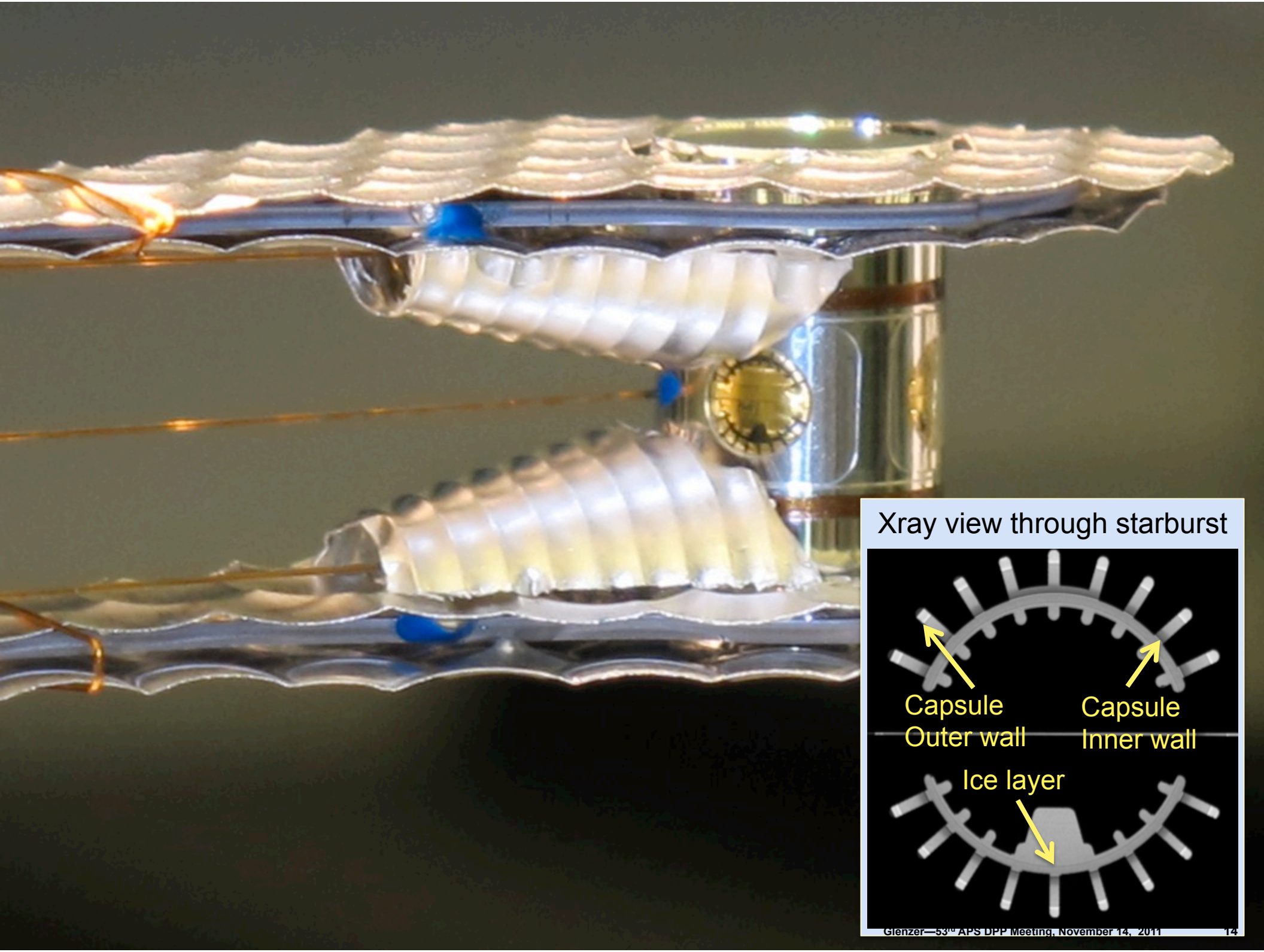
Xray view through starburst
Capsule
Outer wall
Capsule
Inner wall
Ice layer

THD ice layers are characterized in situ and have met specifications on four integrated experiments to date

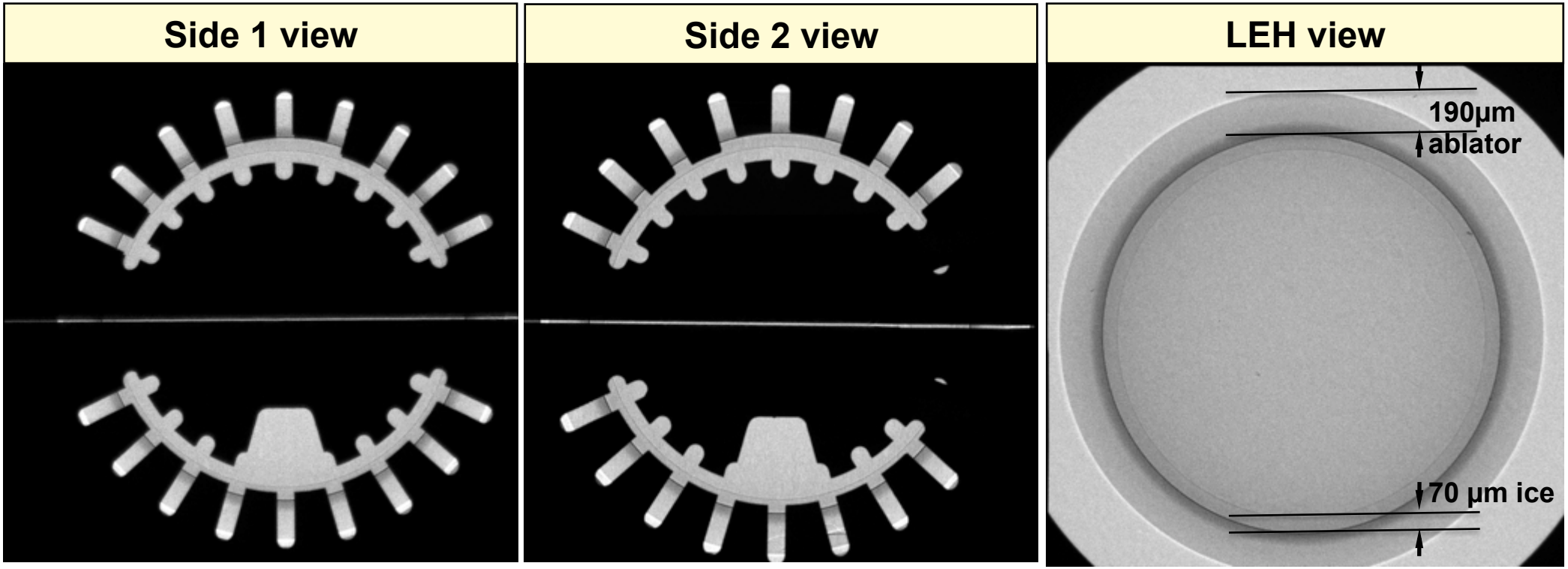

Independent tests have shown that the layer quality is not affected by shroud opening and quench
(cooling from 18.8 K to 17.5 K in last 30s prior to shot)

New high contrast images allows us to estimate projected impact of grooves on the yield of implosions

Local Defects

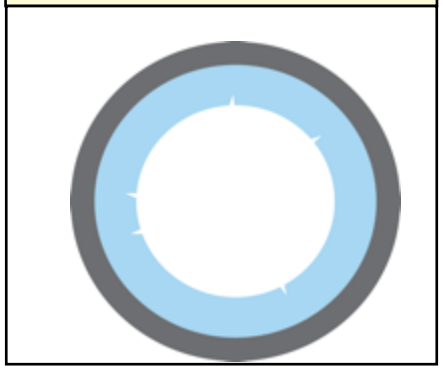

DT1, 5 grooves, Total K = 0.74 μm

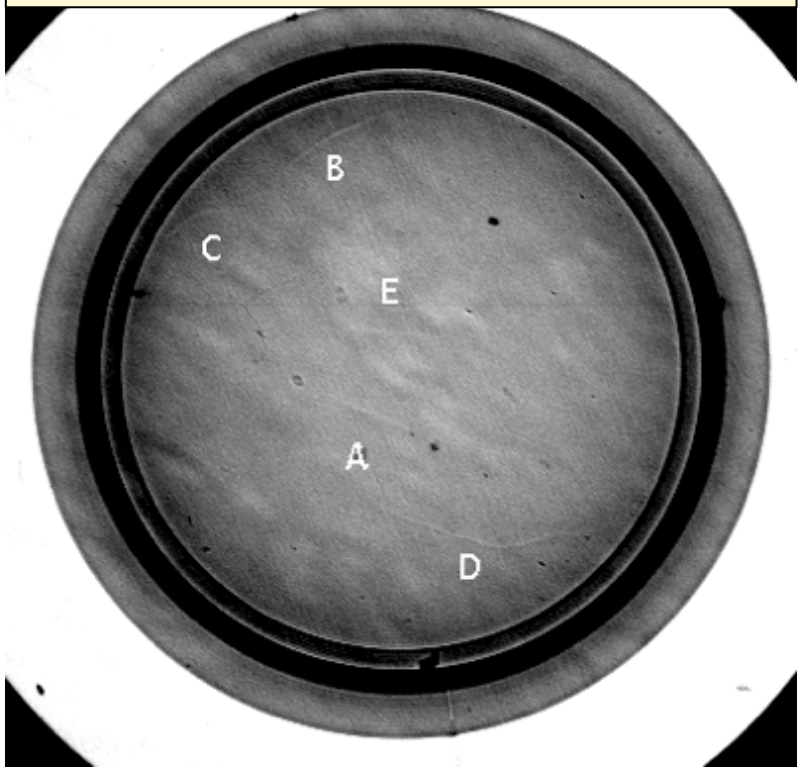

- **Total effect of grooves on hot spot rms sums over all defects**

$$K = \sqrt{\frac{1}{V_{fuel}} \sum_{j=1}^{n} A_j^2 \, L_j}$$

- **To avoid it breaking through the DT layer the area of each defect has been specified**

$$A \leq 200 \ \mu m^2$$

- **Total Yield factor impact**

$$yf = 1.3 - \frac{3}{\sqrt{2}} \left(4.9 \times 10^{-3} nfa^2 + 1.0 \times 10^{-1} K^2 \right)^{\frac{1}{2}}$$

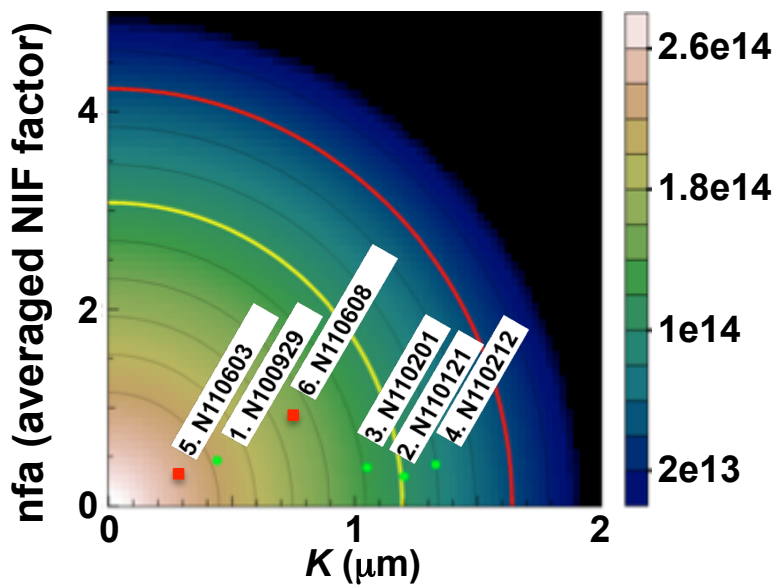

New high contrast images allows us to estimate projected impact of grooves on the yield of implosions

Local Defects

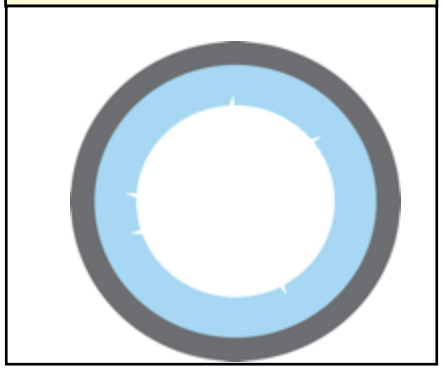

DT1, 5 grooves, Total K = 0.74 μm

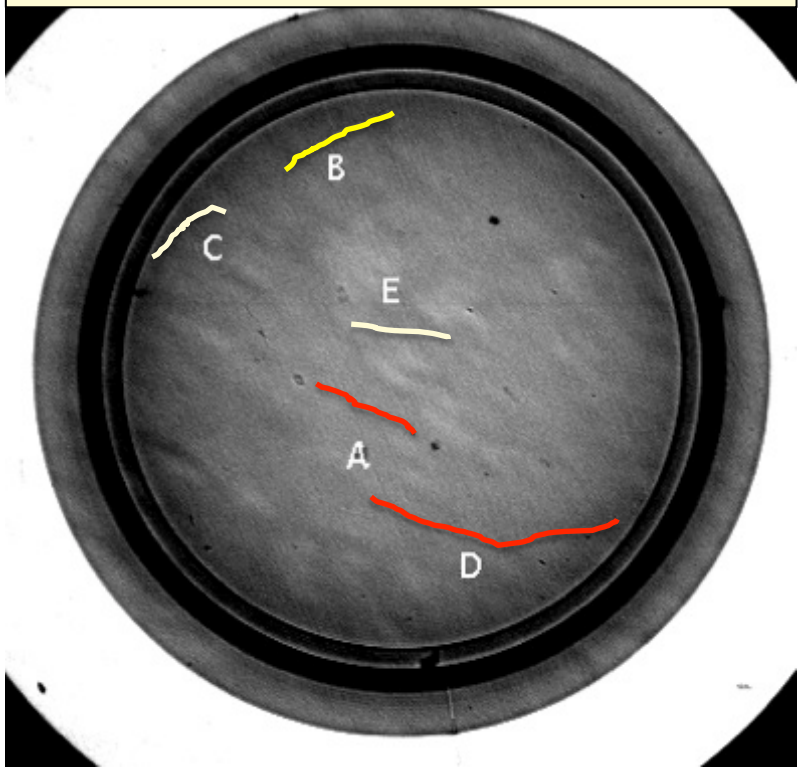

- **Total effect of grooves on hot spot rms sums over all defects**

$$K = \sqrt{\frac{1}{V_{fuel}} \sum_{j=1}^{n} A_j^2 \, L_j}$$

- **To avoid it breaking through the DT layer the area of each defect has been specified**

$$A \leq 200 \ \mu m^2$$

- **Total Yield factor impact**

$$yf = 1.3 - \frac{3}{\sqrt{2}} \left(4.9 \times 10^{-3} nfa^2 + 1.0 \times 10^{-1} K^2 \right)^{\frac{1}{2}}$$

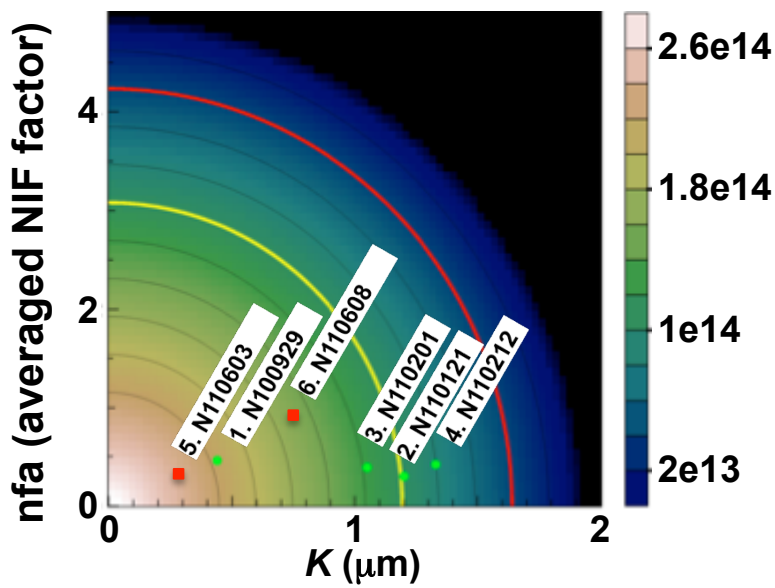

New high contrast images allows us to estimate projected impact of grooves on the yield of implosions

Local Defects

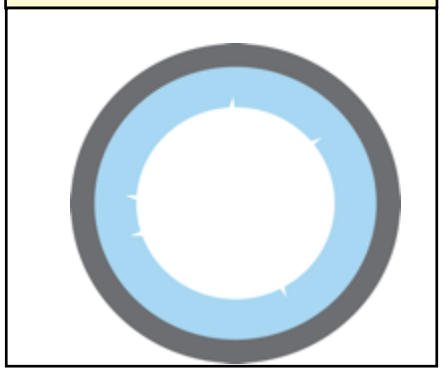

DT2, 1 groove, Total K = 0.11 μm

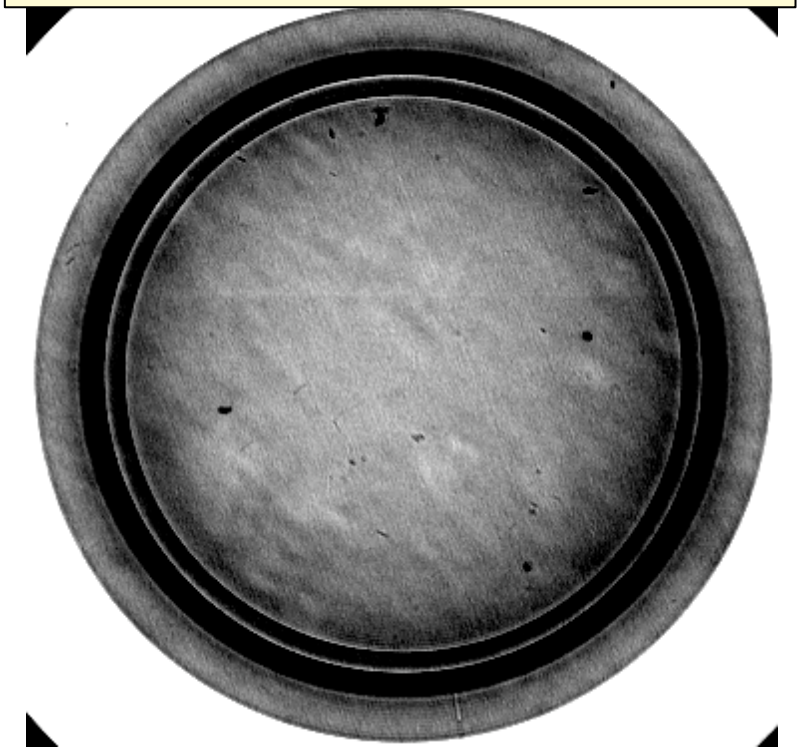

- **Total effect of grooves on hot spot rms sums over all defects**

$$K = \sqrt{\frac{1}{V_{fuel}} \sum_{j=1}^{n} A_j^2 \, L_j}$$

- **To avoid it breaking through the DT layer the area of each defect has been specified**

$$A \leq 200 \ \mu m^2$$

- **Total Yield factor impact**

$$yf = 1.3 - \frac{3}{\sqrt{2}} \left(4.9 \times 10^{-3} nfa^2 + 1.0 \times 10^{-1} K^2 \right)^{\frac{1}{2}}$$

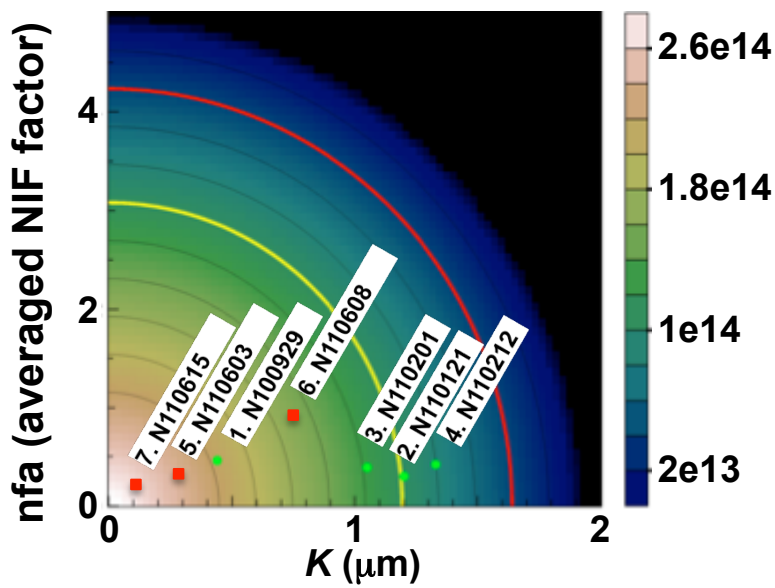

We are assessing hot spot formation and thermonuclear fuel assembly with accurate measurements of neutron yield and the down-scattered ratio

LBL, SNL, LLNL Neutron Activation

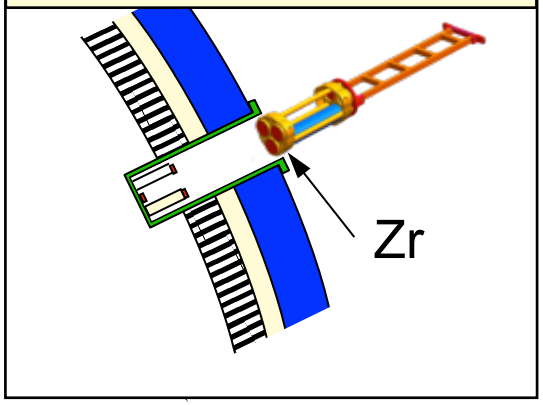

14.1 MeV DT Yield

$$dsr = \left(\frac{10-12\ MeV}{13-15\ MeV}\right) \propto \rho R$$

Burn width

MIT, LLE Magnetic Recoil Spectrometer (MRS)

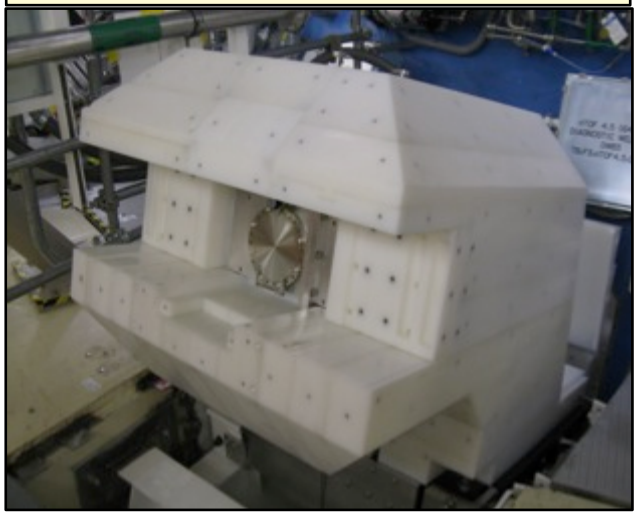

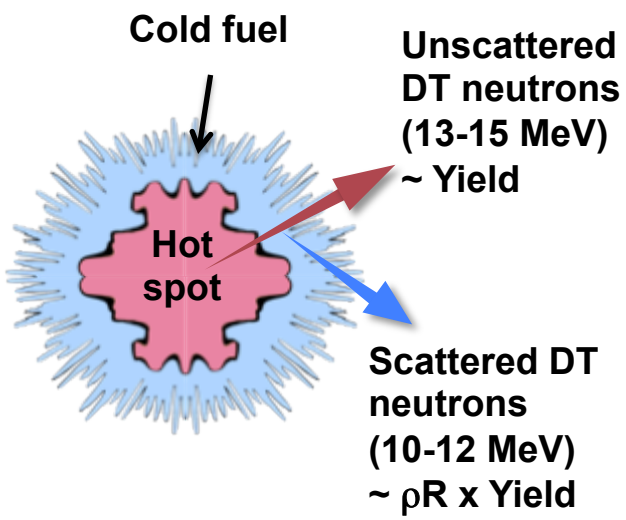

LLE, LLNL Neutron Time of Flight (NToF)

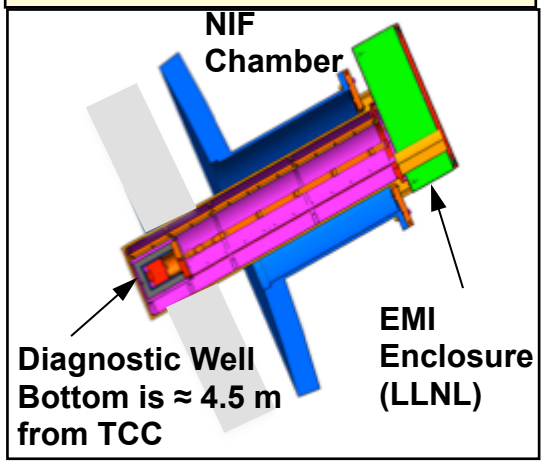

Yield and dsr accuracy requirements
<10% at $Y_n > 10^{14}$

LANL Gamma Reaction History (GRH)

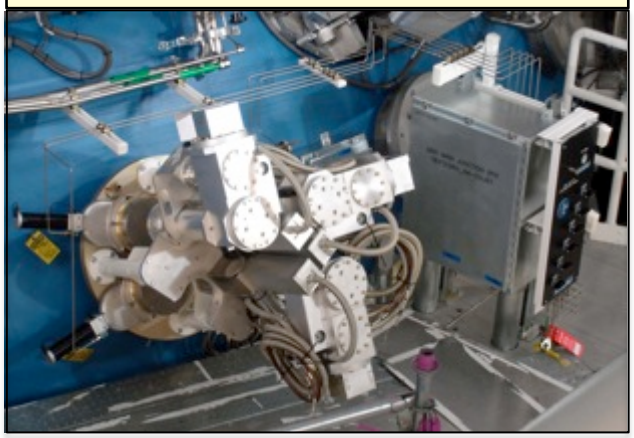

NADS: Zr Well_NAD measures yield for DT shots to absolute accuracy of ± 7%

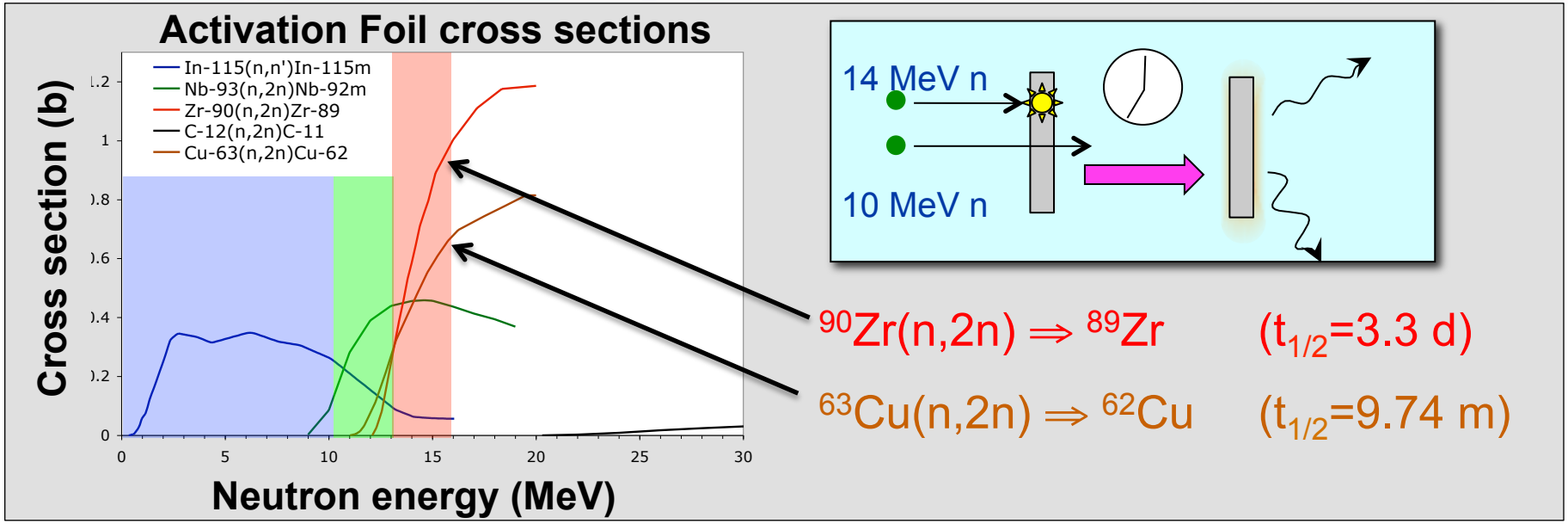

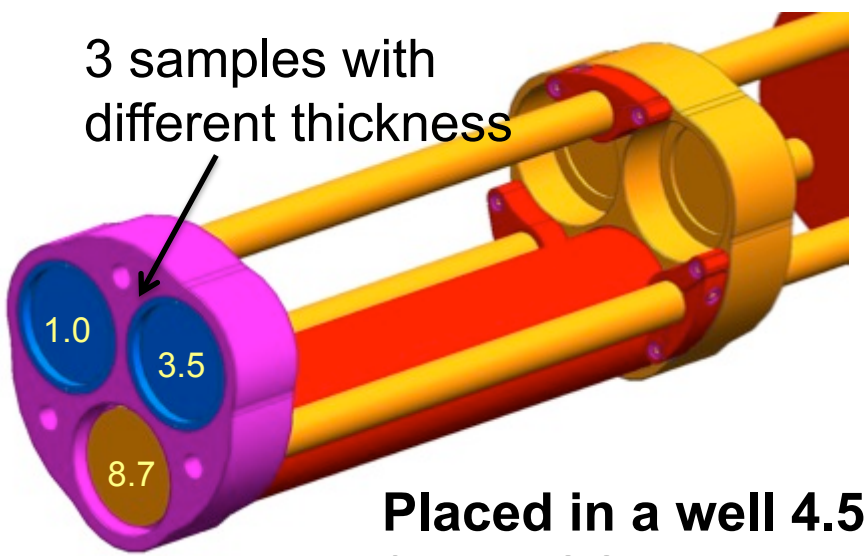

Placed in a well 4.5m from TCC

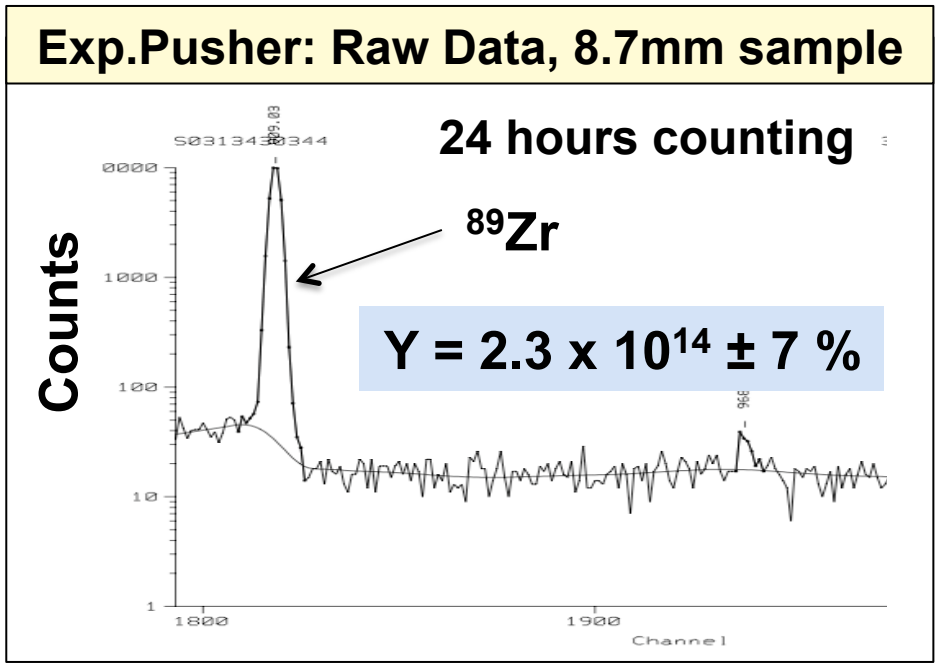

NTOF: THD Neutron Time of Flight measurements provide total yield (< 10%), nuclear bang time (± 30 ps) and burn averaged ion temperature (± 5-10%)

NTOF [scintillator/photodetector] sensitivity to ion temperature

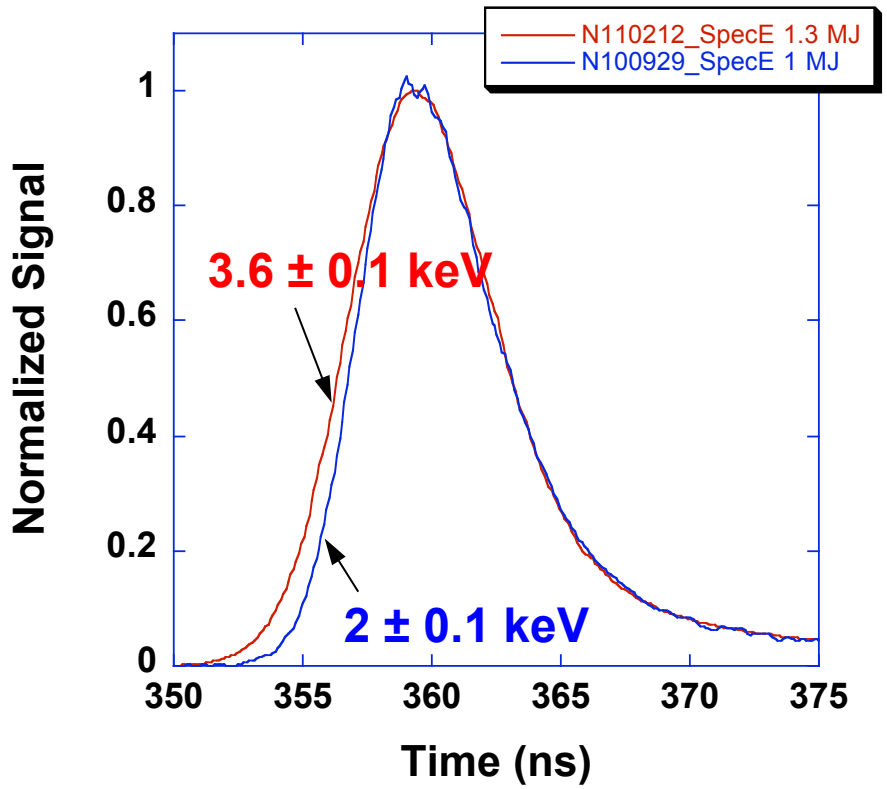

Absolute error: 7% (NADS), 5% (MRS)
Error in the weighted mean is 2.1%

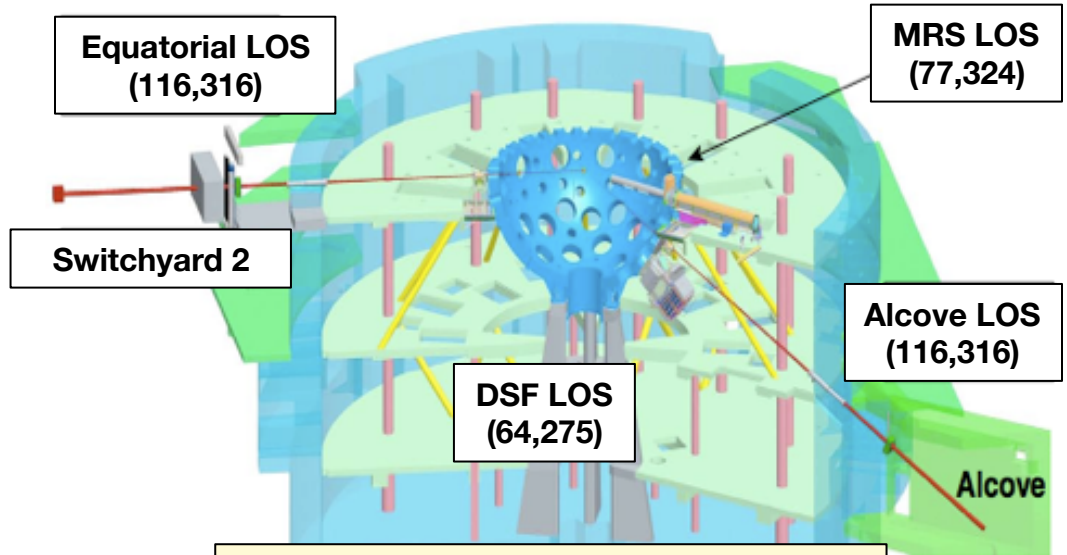

Yield is 1.2 (± 2.1%) x 10^{14}

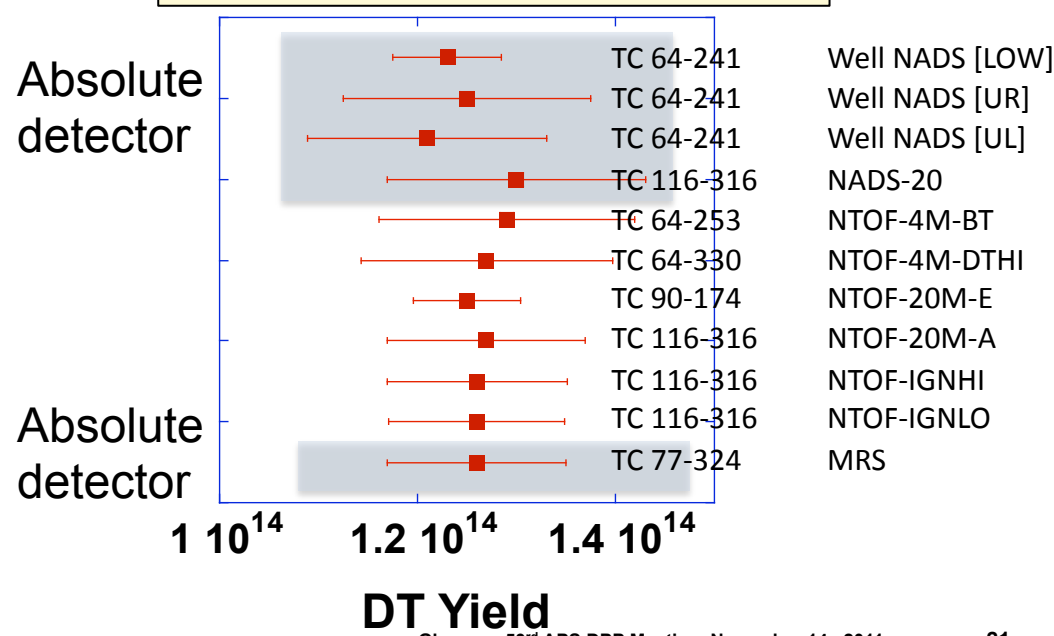

MRS: A *down scattered ratio* of is measured with high accuracy of ± 0.003 using the MRS spectrum

n (14.1 MeV) + D
→ n' (~1.6 MeV) + d' (~12.5 MeV)

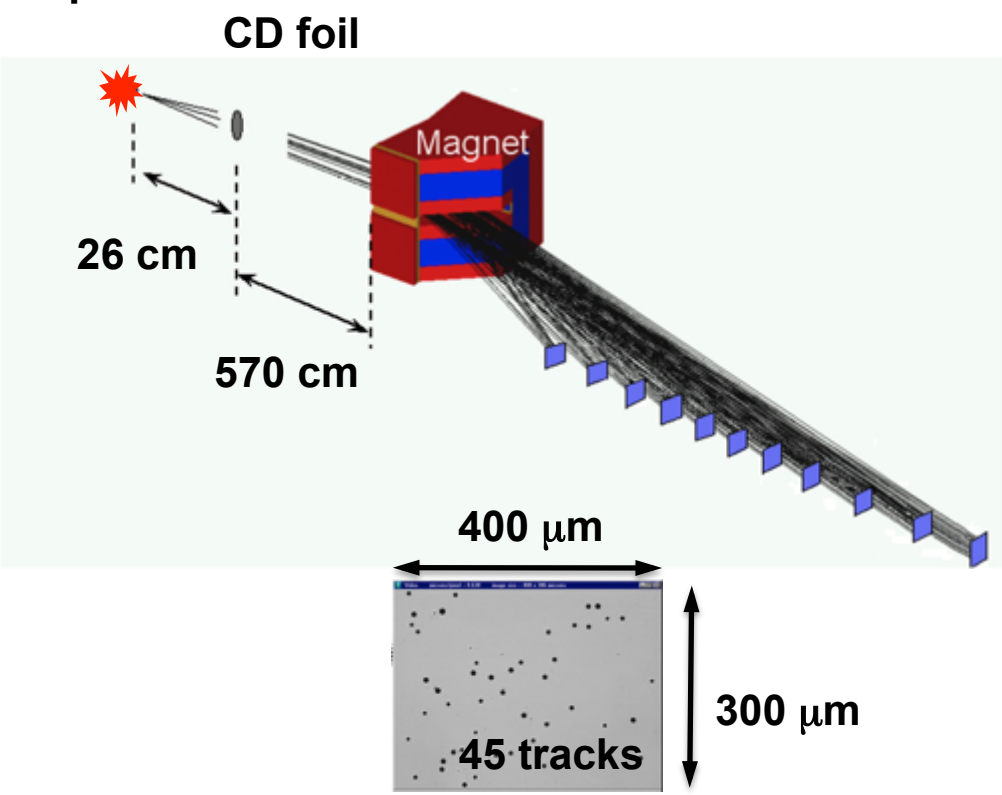

Magnetic Recoil Spectrometer (MRS)

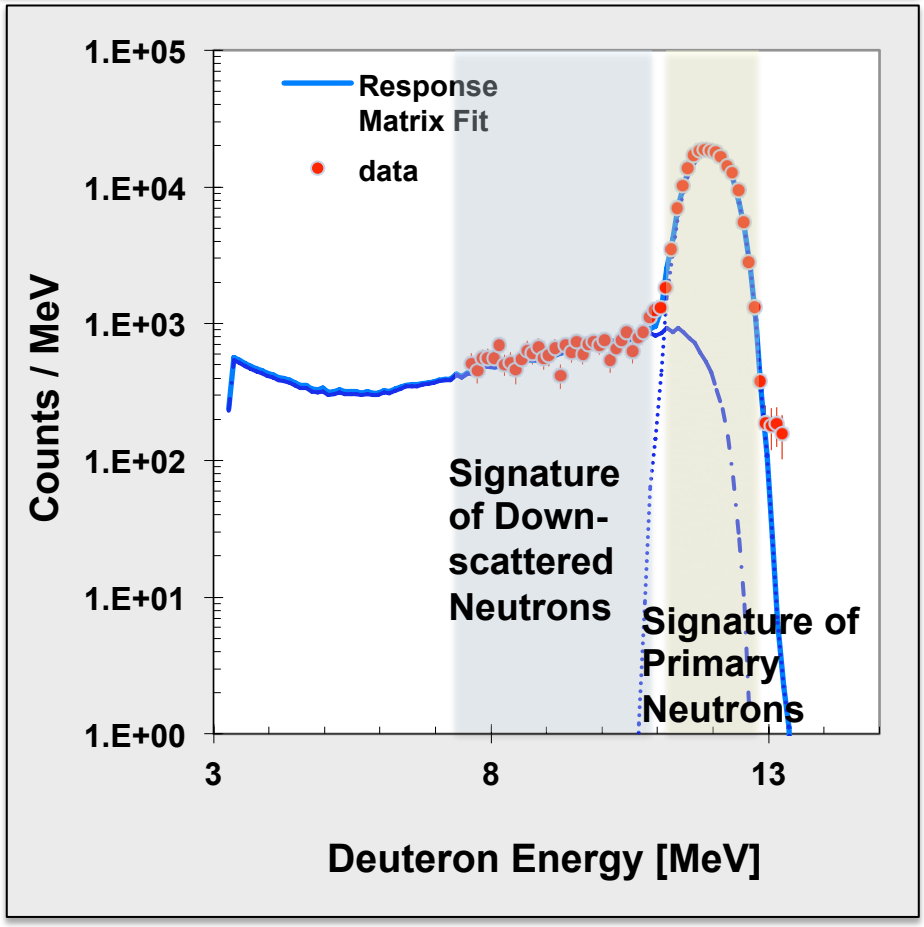

Deuterons counted at 7 – 10 MeV indicate neutron energy loss in the dense shell that is surrounding the hot spot

GRH: THD Gamma-ray spectrum has been measured providing nuclear bang time (± 30 ps) and burn width (± 30 ps)

Calculated THD γ-Ray Spectrum

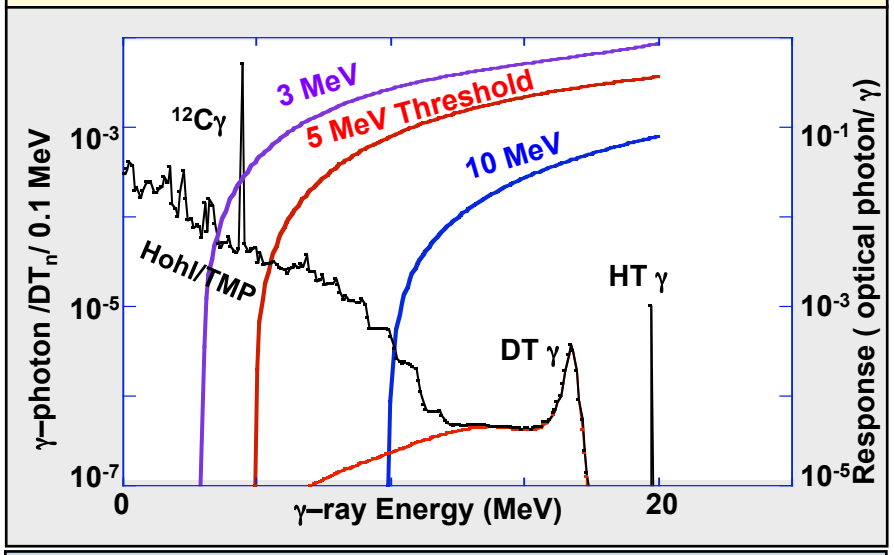

Energy threshold measurements:

- DT (+HT) Yield
- Ablator Areal Density

Measured THD signals

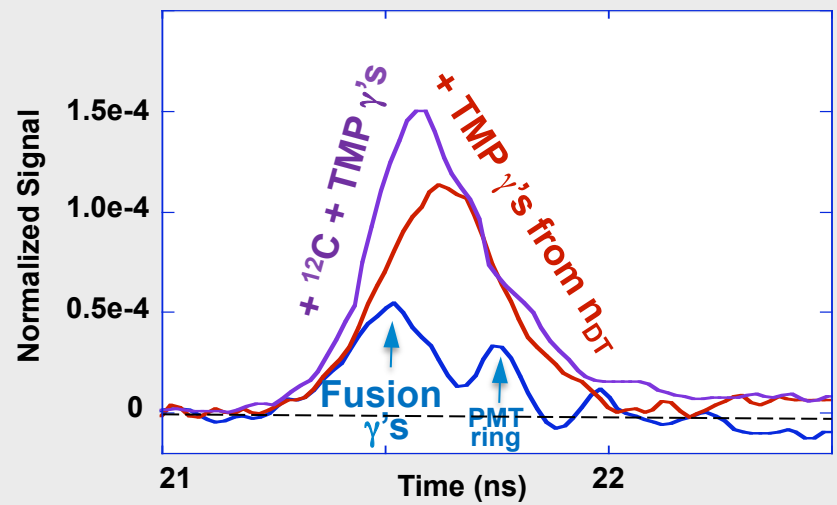

Burn width of 190 ps
^{12}C signal clearly observable

- 10 MeV representative of Fusion Gammas (DT-γ & HT-γ)
- 5 MeV also includes neutron-induced γ-rays off Thermomechanical Package (TMP)
  - tracks fusion gammas until neutrons reach TMP (~100 ps delay)
- 3 MeV also includes 4.44 MeV 12C(n,n') γ-rays
  - Difference between 3 & 5 MeV representative of 4.44 MeV 12C(n,n') γ-rays
  - Roughly synchronous with fusion gammas

During commissioning, THD fuel ρr was 2.5x below ignition spec and ITFx had only reached 0.02

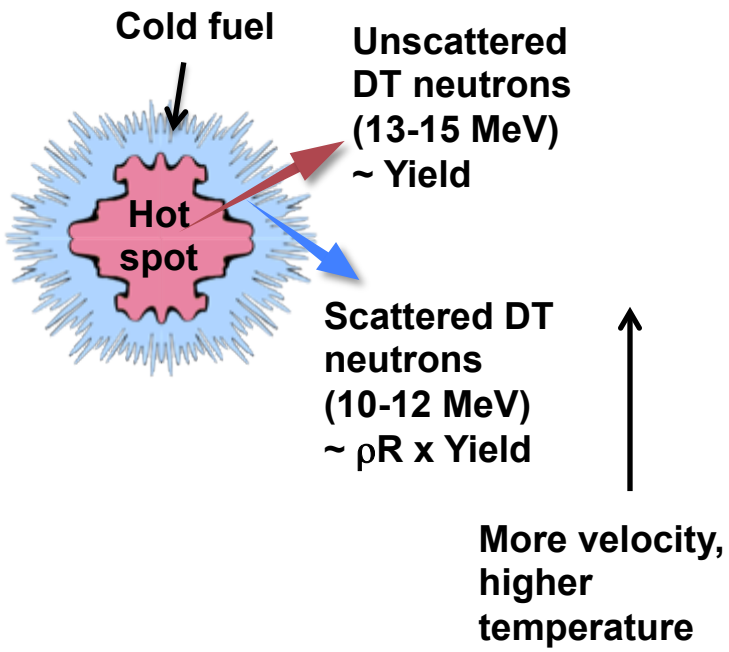

$$\mathrm{ITFx} = \left(\frac{Yield}{3.2e15}\right)\left(\frac{dsr}{.07}\right)^{2.3}$$

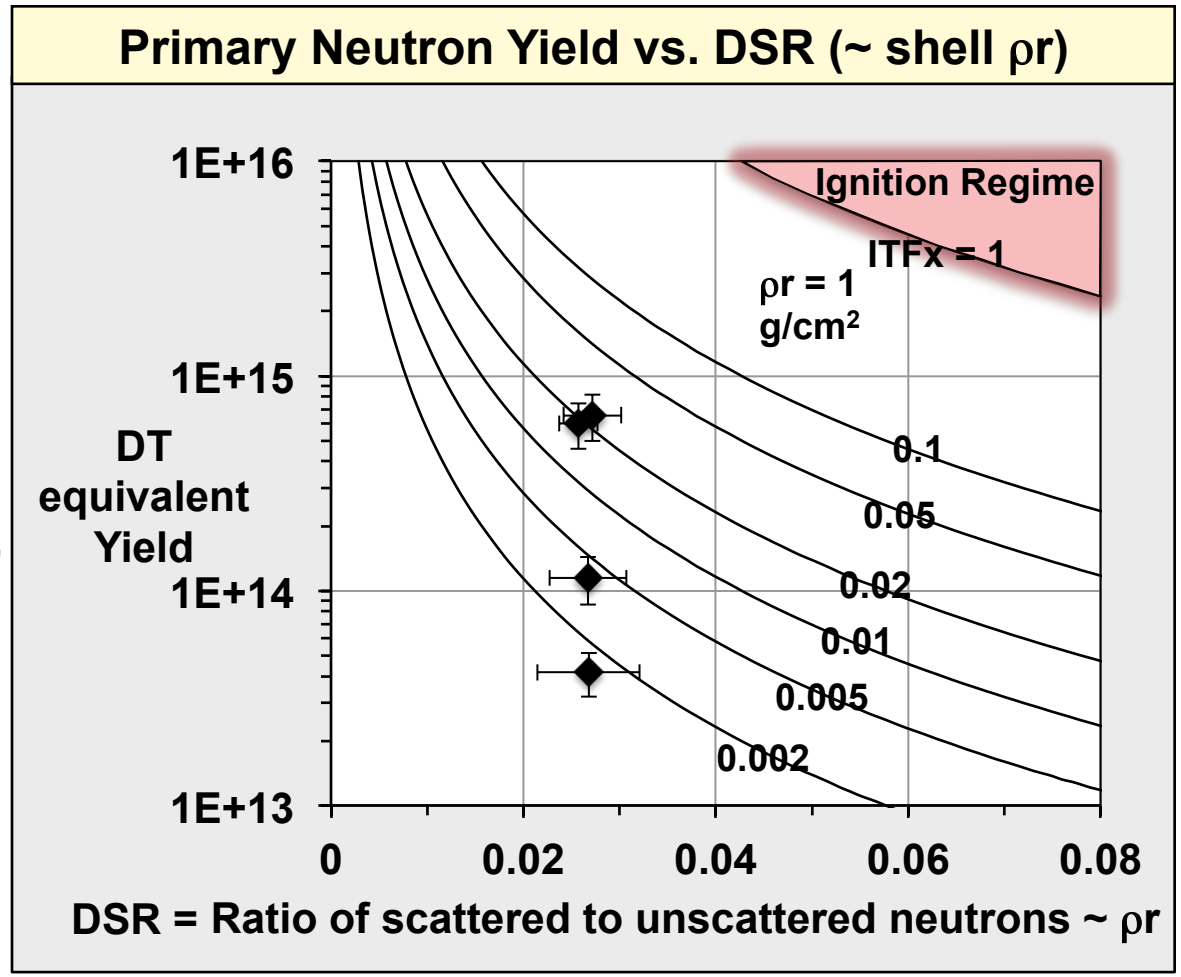

More compression, higher density →

To optimize the target for ignition we will adjust velocity, adiabat, mix and shape

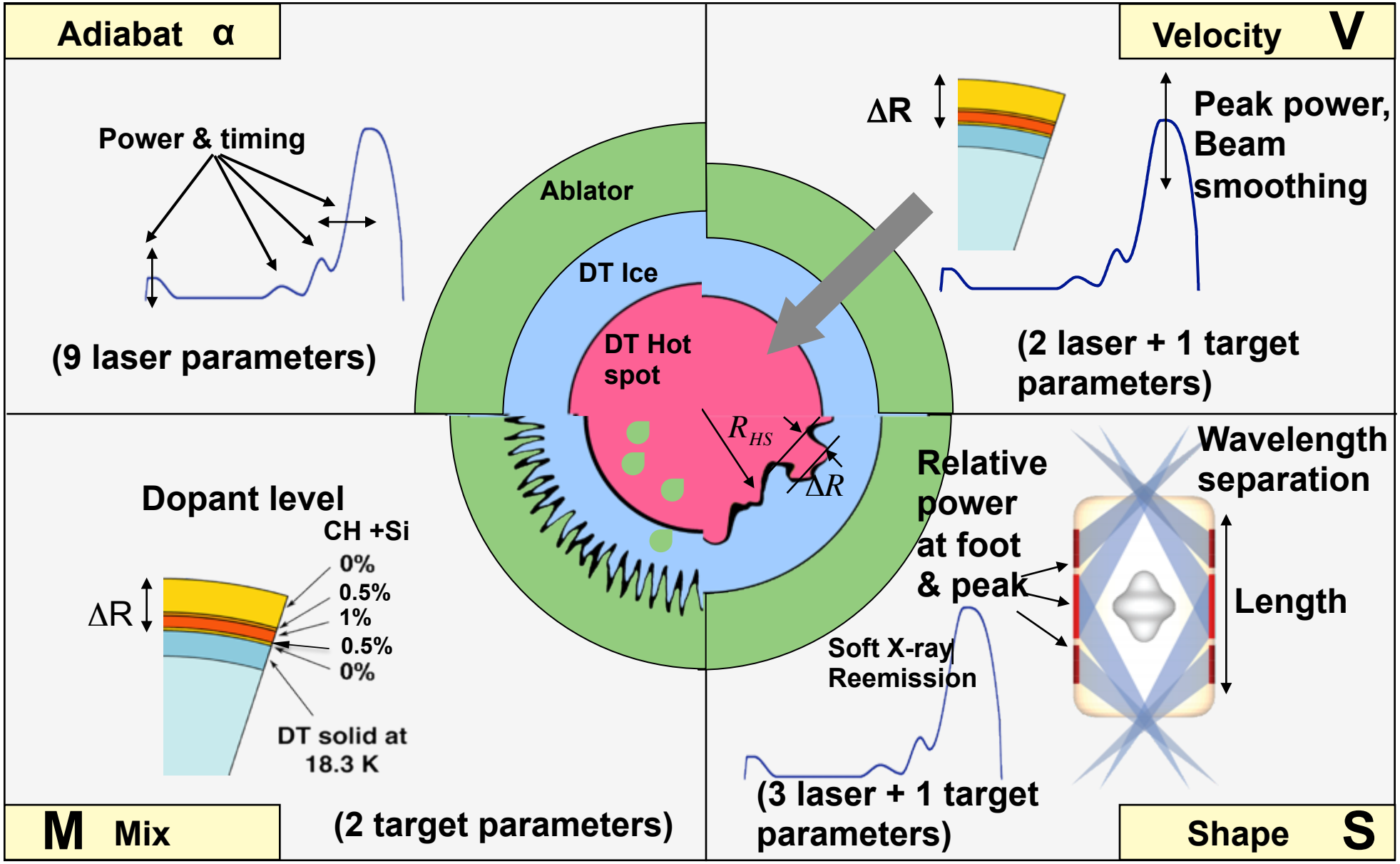

We use a variety of now fully validated targets to tune the capsule shape, adiabat, velocity and mix

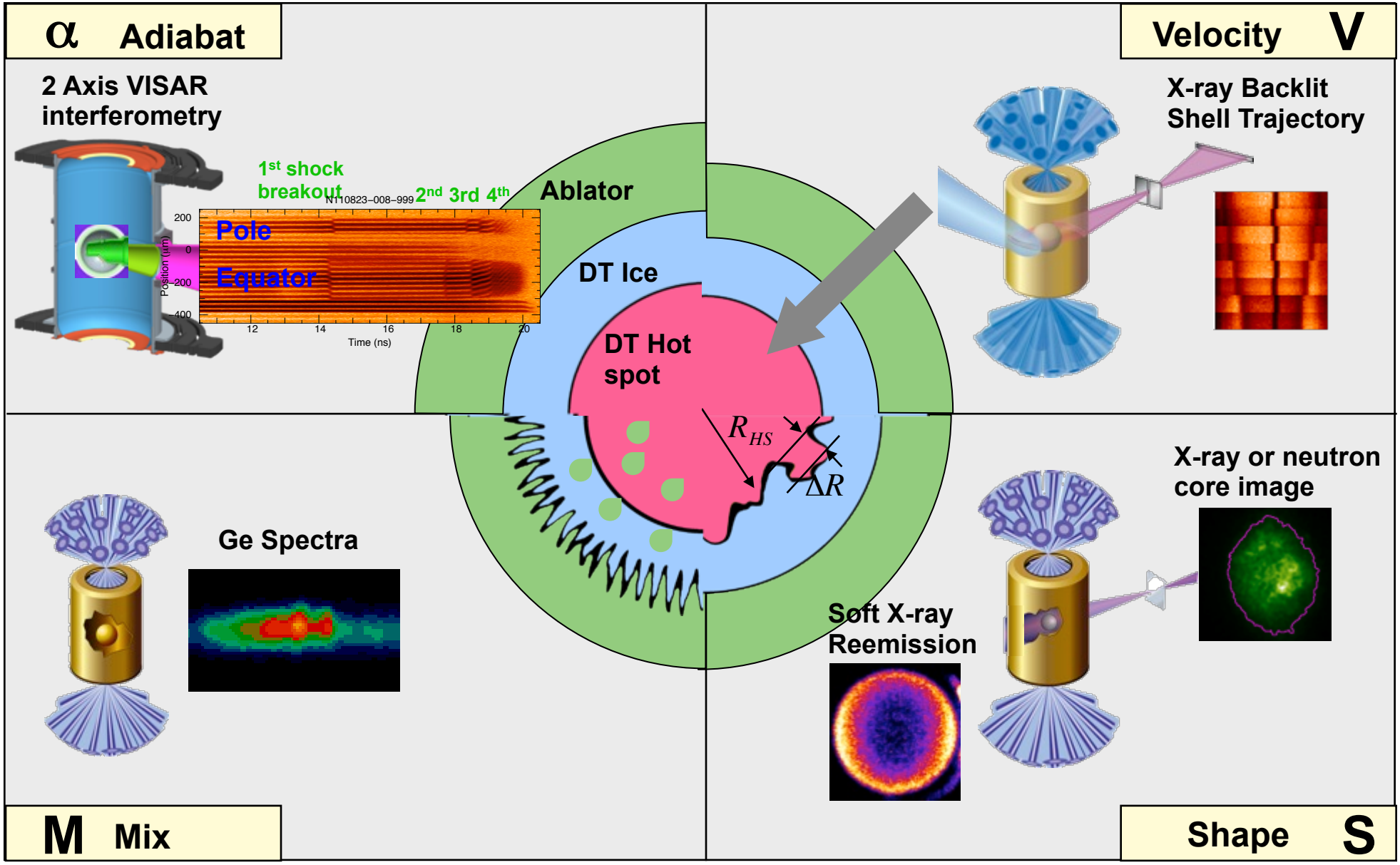

Using tuned pulse (through shock timing), THD and DT fuel ρr improved by ≈ 2x, and ITFx improved to 0.06

Pulse shape changes

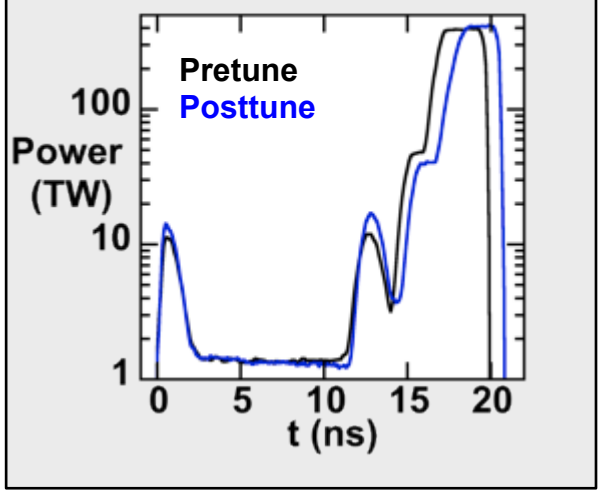

MRS data

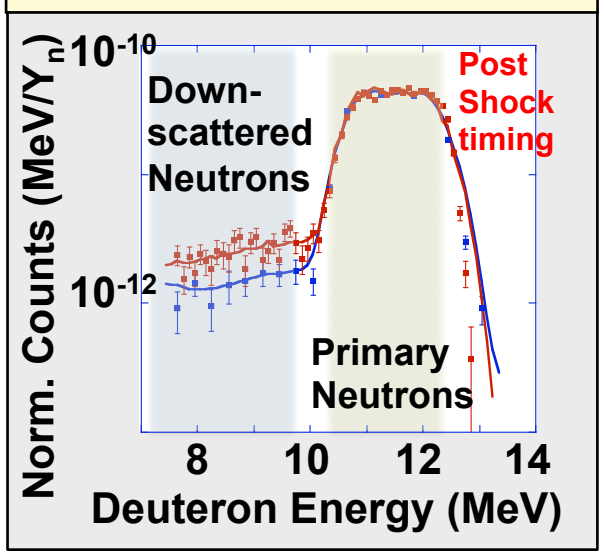

Primary Neutron Yield vs. DSR (~ shell ρr)

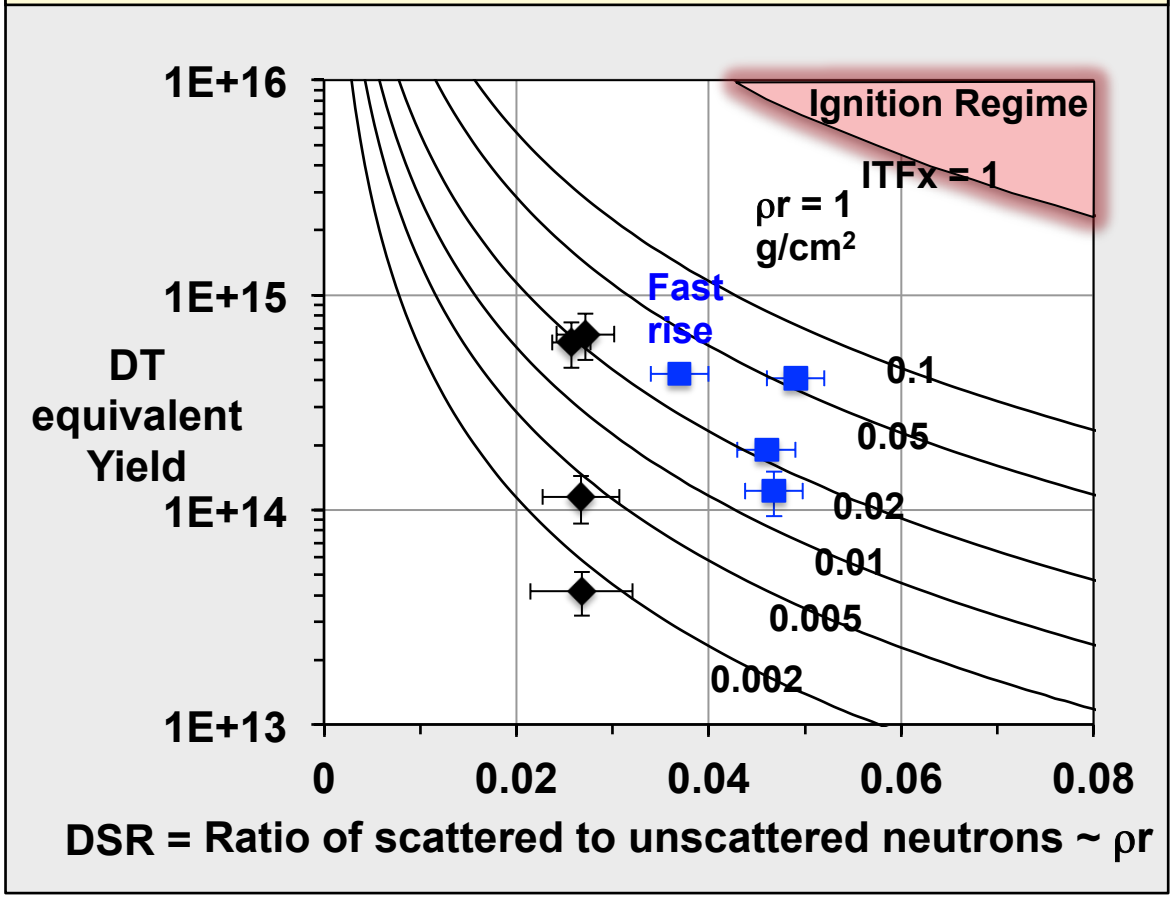

To improve velocity and shape we have recently moved to a new scale 575 hohlraum and Si ablator

Tuning shape of a Si-doped capsule implosion in 5.75 mm diameter hohlraum required three laser wavelengths

DT implosion performance is dependent on M-modes that have been tuned with λ_3

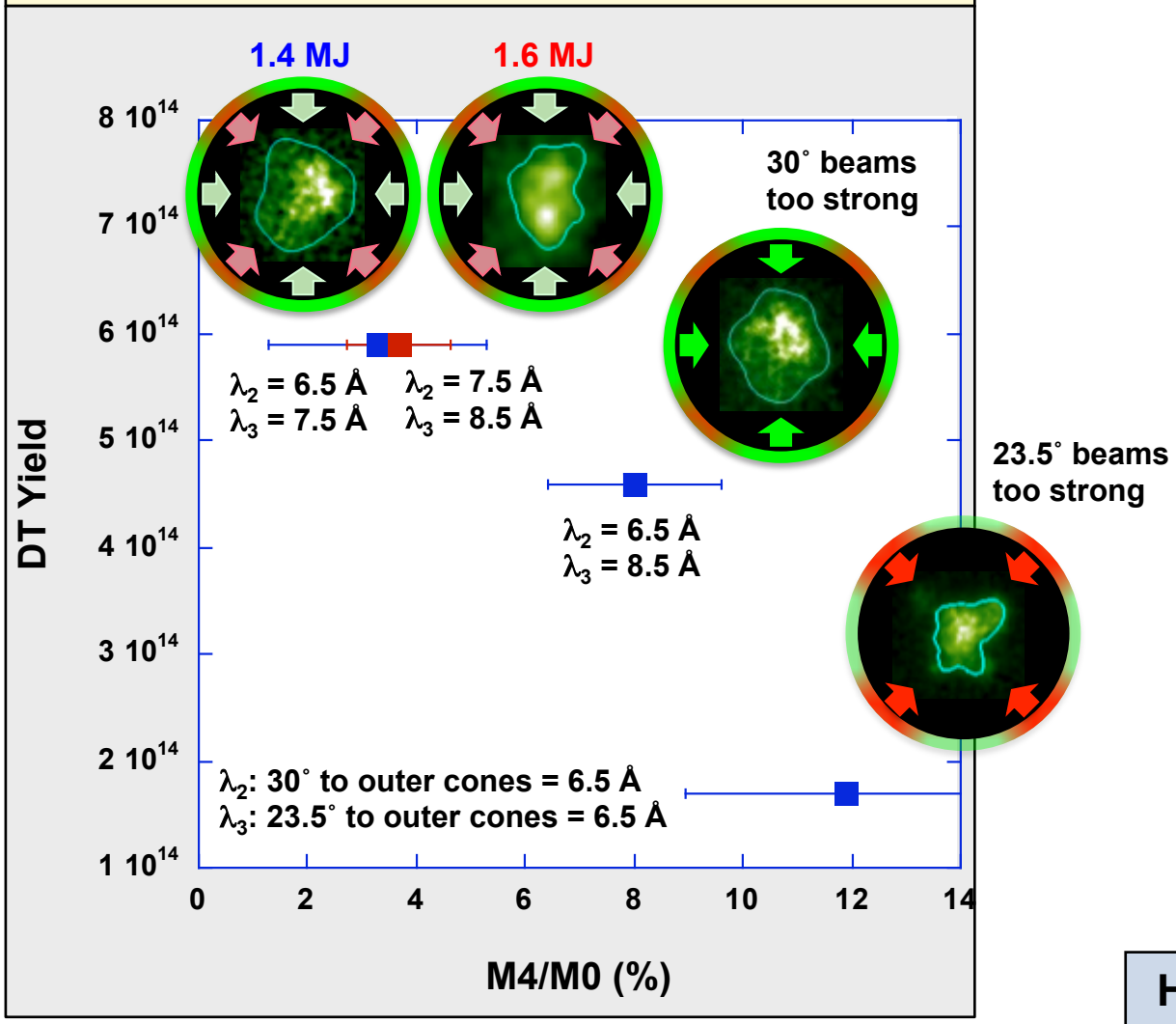

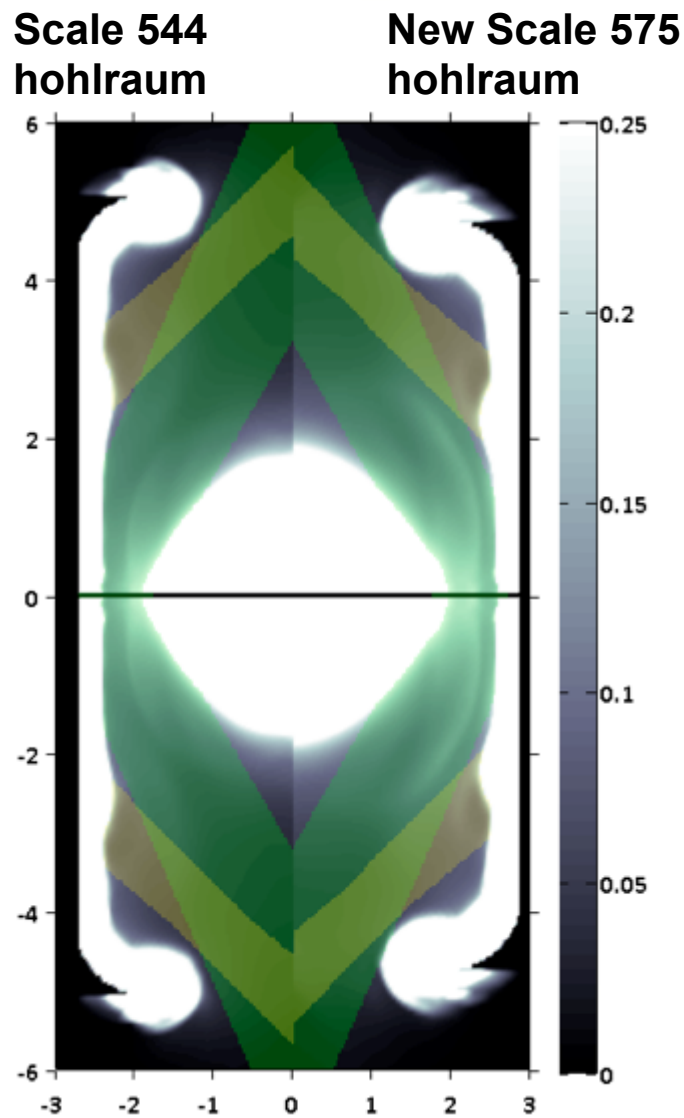

Hohlraum allows shape tuning with the potential for high velocity

A shock-timed Si-doped capsule implosion in 5.75 mm diameter hohlraum reached an ITFx of 0.1

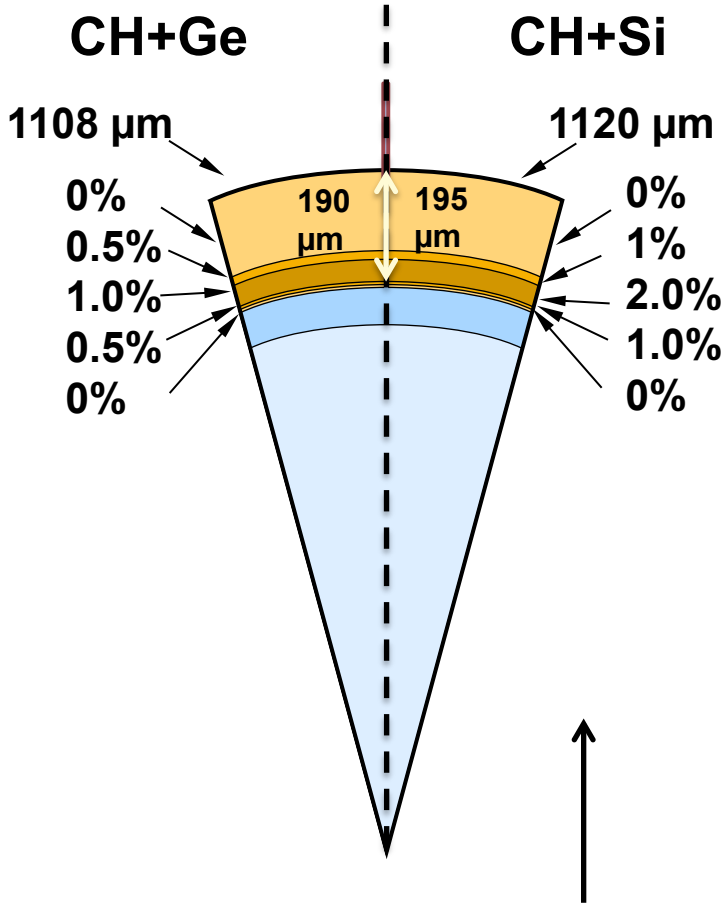

More velocity, higher temperature

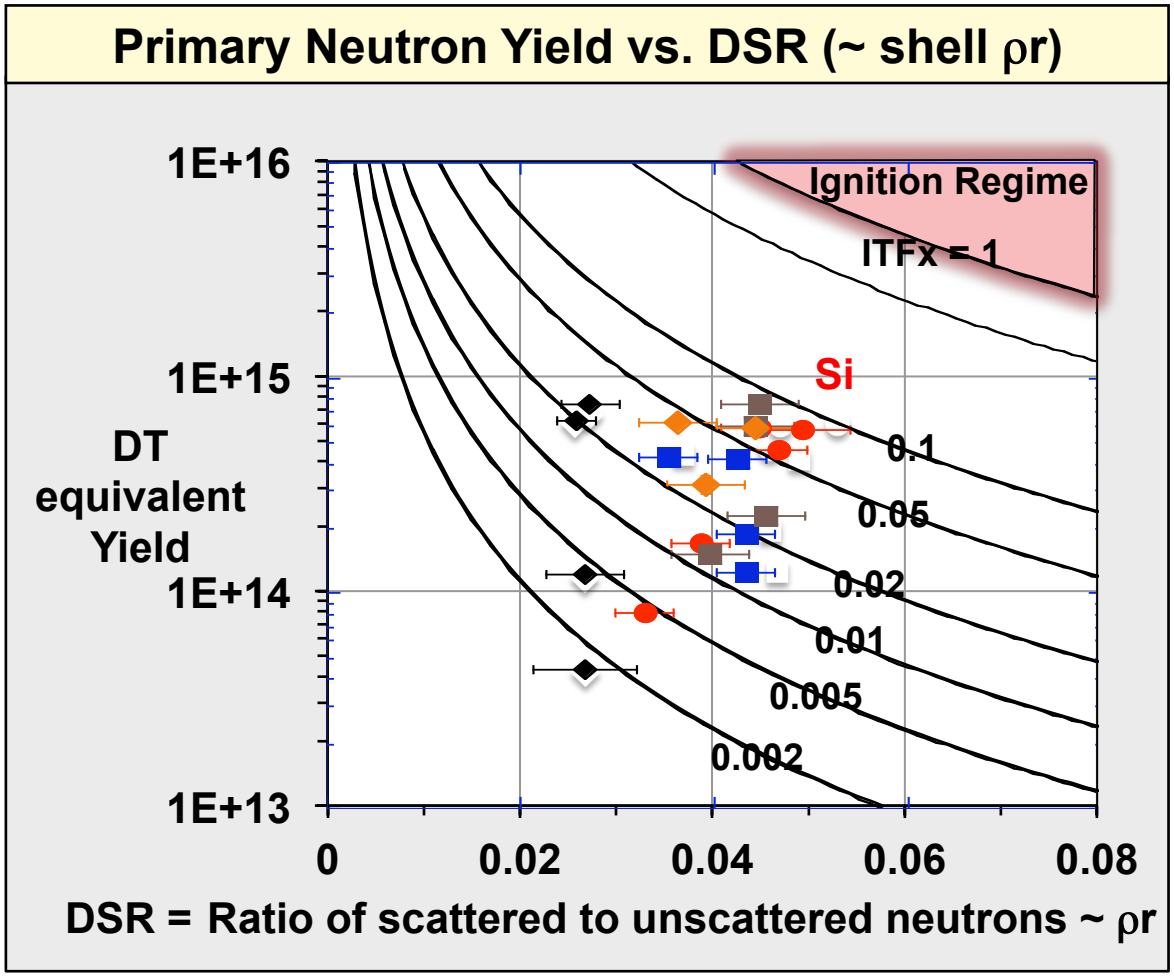

More compression, higher density

We are currently performing a shape tuning campaign to fully explore the regime between ITFx ~ 0.1 and 1

Shell areal density and absolute x-ray emission measurements indicate ultrahigh pressures

First analysis of Neutron Imaging data suggest high density shell

Primary Neutrons 13-17 MeV

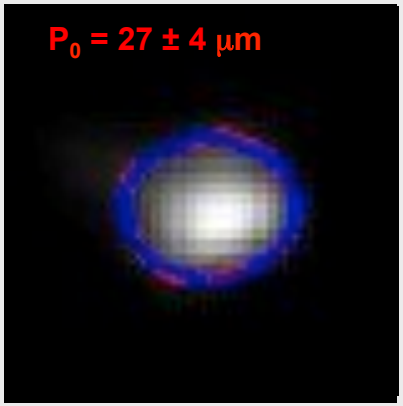

Down scattered Neutrons 10-12 MeV

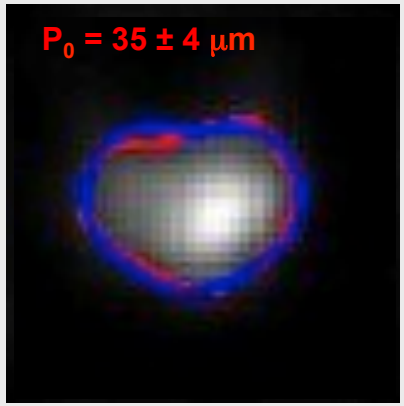

Absolute X-ray emission

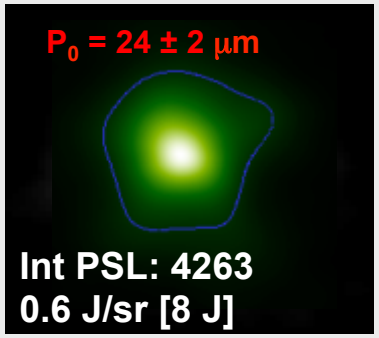

$P_{br} \sim \rho^2 T^{1/2}$
$T = 3.6$ keV [ntof]
$n_e = 8 \times 10^{24}$ cm^{-3}

Tuning has improved shell ρR to high level areal densities

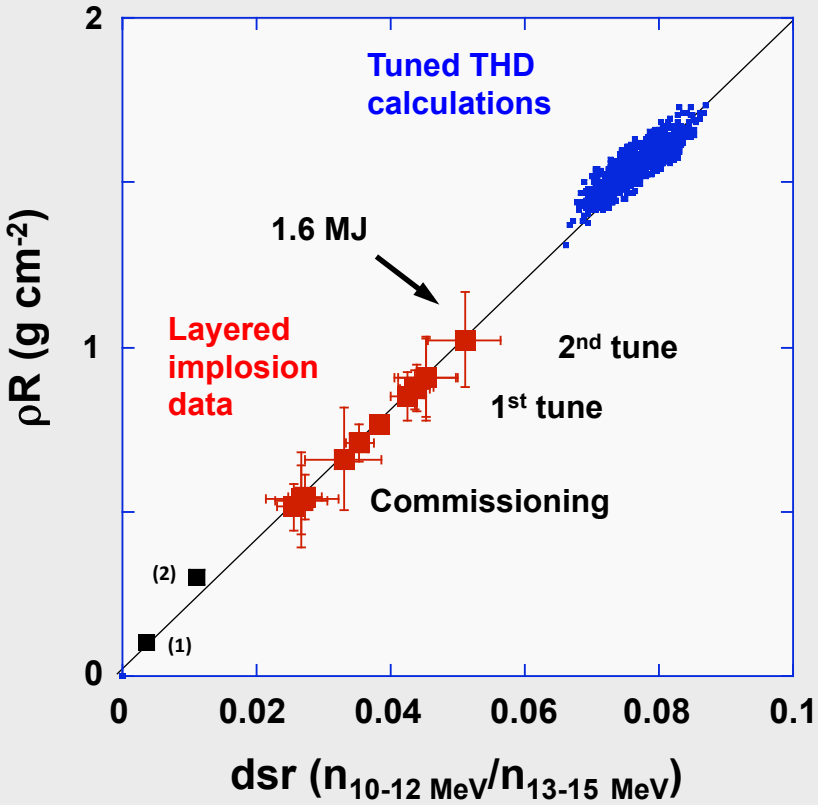

— Burn time of 120 - 150 ps

(1) Azechi et al., Laser and Particle Beams (1991) 9, 193-207
(2) Goncharov et al., Physics Review Letters (2010) 104, 165001

Shell areal density and absolute x-ray emission measurements indicate ultrahigh pressures

First analysis of Neutron Imaging data suggest high density shell

Primary Neutrons 13-17 MeV

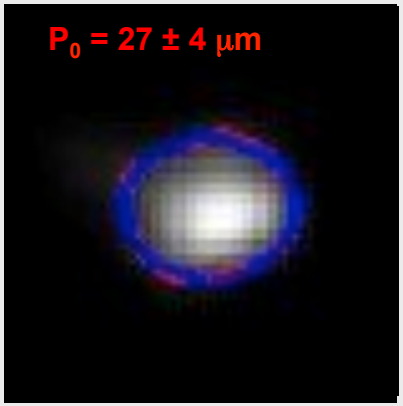

Down scattered Neutrons 10-12 MeV

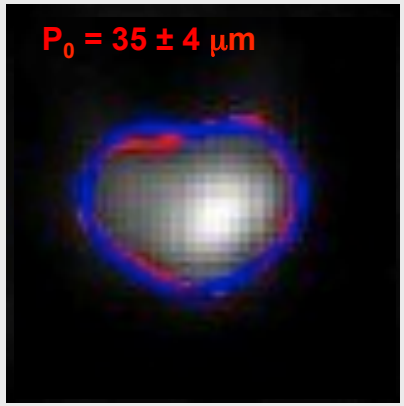

Absolute X-ray emission

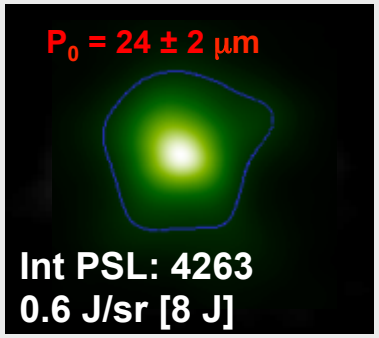

$P_{br} \sim \rho^2 T^{1/2}$
T = 3.6 keV [ntof]
$n_e = 8 \times 10^{24}$ cm^{-3}

— Burn time of 120 - 150 ps

- Fuel pressure estimate
  - $\rho R = 1$ g cm^{-2}
  - $\Delta R = 0.0011 – 0.0017$ cm
  - $\rho = 550$ g cm^{-3}
  - $n_e = \rho/2.5\ m_p = 10^{26}$ cm^{-3}
  - P_{fermi} (~ $\rho^{5/3}$) = 80 Gbar
  - $P\tau \sim 10$ atm-s
- Hot spot pressure
  - $n_e = 8 \times 10^{24}$ cm^{-3}
  - <T> = 3.6 keV
  - P = 92 Gbar
  - $P\tau \sim 12$ atm-s
- For comparison, the Joint European Tokamak and Omega have produced
  - $P\tau \sim 1$ atm-s

NIF implosions show record values of the Lawson fusion criterion

- First NIF indirect drive cryogenic implosion (commissioning)
  - $\rho R = 0.5$ g cm^{-2}
  - $\langle T \rangle = 2.5$ keV
  - $P\tau \sim 1$ atm-s
- NIF implosion after initial tuning
  - $\rho R = 1$ g cm^{-2}
  - $\langle T \rangle = 3$ keV
  - $P\tau \sim 10$ atm-s
- Omega (2009) produced
  - $P\tau \sim 1$ atm-s
- For comparison, the Joint European Tokamak has produced
  - $P\tau \sim 1$ atm-s

R. Betti et al., PHYS. PLASMAS 17, 058102 (2010) with data from J. P. Freidberg MIT.

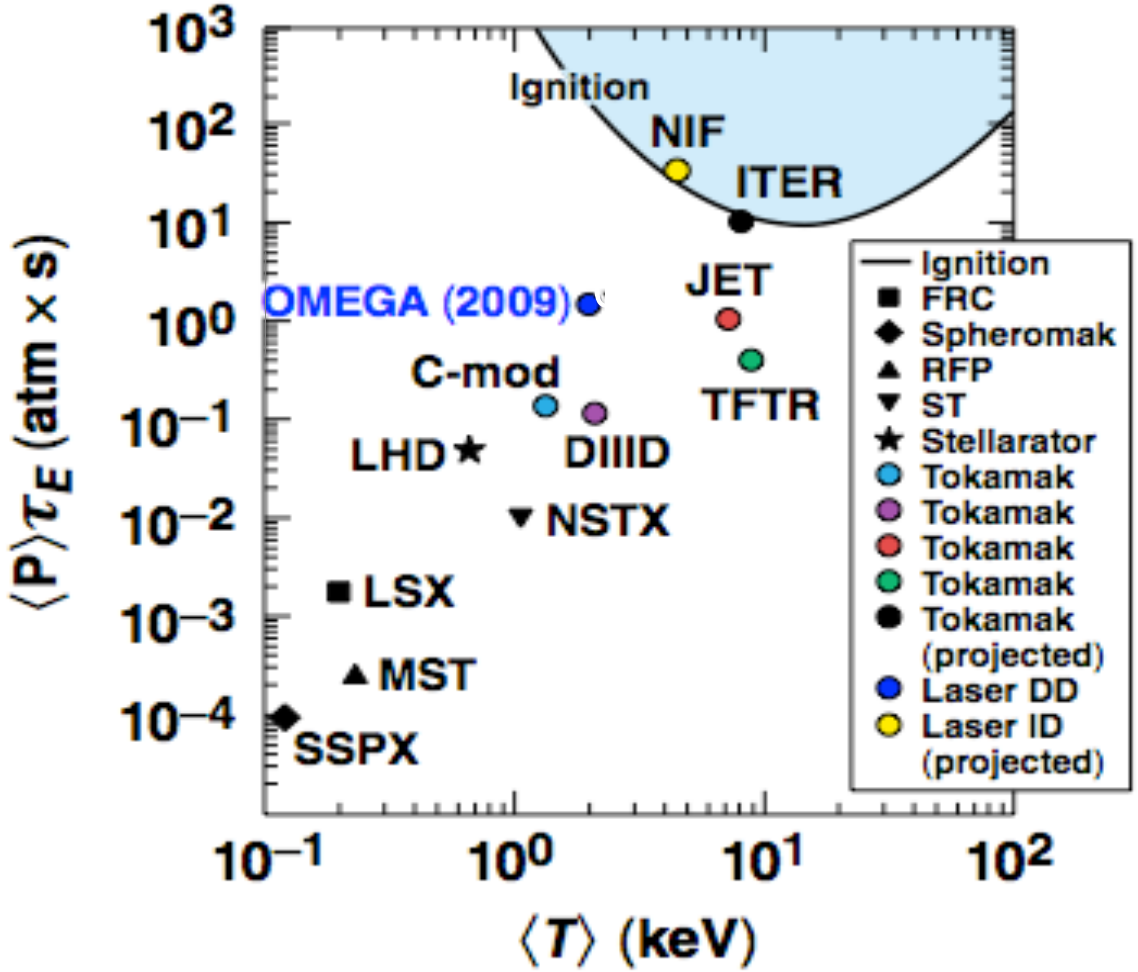

NIF implosions show record values of the Lawson fusion criterion

- First NIF indirect drive cryogenic implosion (commissioning)
  - $\rho R = 0.5$ g cm^{-2}
  - $\langle T \rangle = 2.5$ keV
  - $P\tau \sim 1$ atm-s
- NIF implosion after initial tuning
  - $\rho R = 1$ g cm^{-2}
  - $\langle T \rangle = 3$ keV
  - $P\tau \sim 10$ atm-s
- Omega (2009) produced
  - $P\tau \sim 1$ atm-s
- For comparison, the Joint European Tokamak has produced
  - $P\tau \sim 1$ atm-s

R. Betti et al., PHYS. PLASMAS 17, 058102 (2010) with data from J. P. Freidberg MIT.

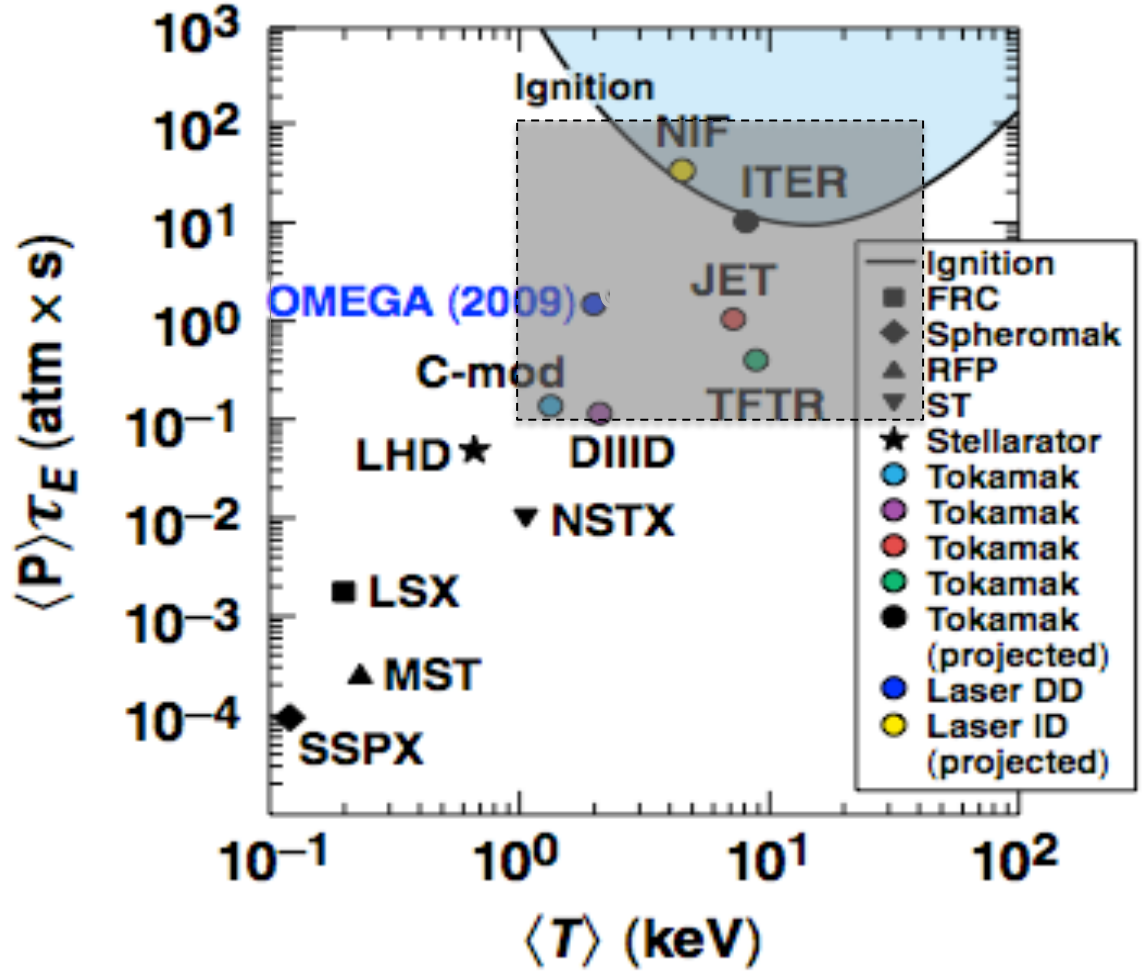

NIF implosions show record values of the Lawson fusion criterion

- First NIF indirect drive cryogenic implosion (commissioning)
  - $\rho R = 0.5$ g cm^{-2}
  - $\langle T \rangle = 2.5$ keV
  - $P\tau \sim 1$ atm-s
- NIF implosion after initial tuning
  - $\rho R = 1$ g cm^{-2}
  - $\langle T \rangle = 3$ keV
  - $P\tau \sim 10$ atm-s
- For comparison, the Joint European Tokamak and Omega have produced
  - $P\tau \sim 1$ atm-s

NIF implosions approach ignition regime

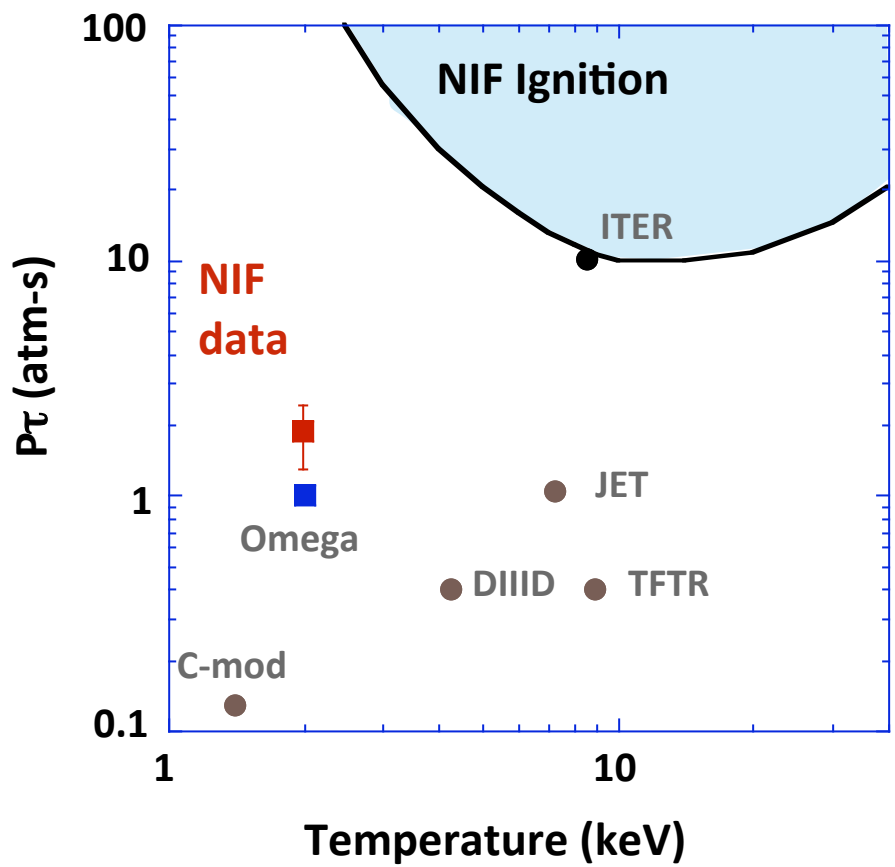

NIF implosions show record values of the Lawson fusion criterion

- First NIF indirect drive cryogenic implosion (commissioning)
  - $\rho R = 0.5$ g cm^{-2}
  - $\langle T \rangle = 2.5$ keV
  - $P\tau \sim 1$ atm-s
- NIF implosion after initial tuning
  - $\rho R = 1$ g cm^{-2}
  - $\langle T \rangle = 3$ keV
  - $P\tau \sim 10$ atm-s
- For comparison, the Joint European Tokamak and Omega have produced
  - $P\tau \sim 1$ atm-s

NIF implosions approach ignition regime

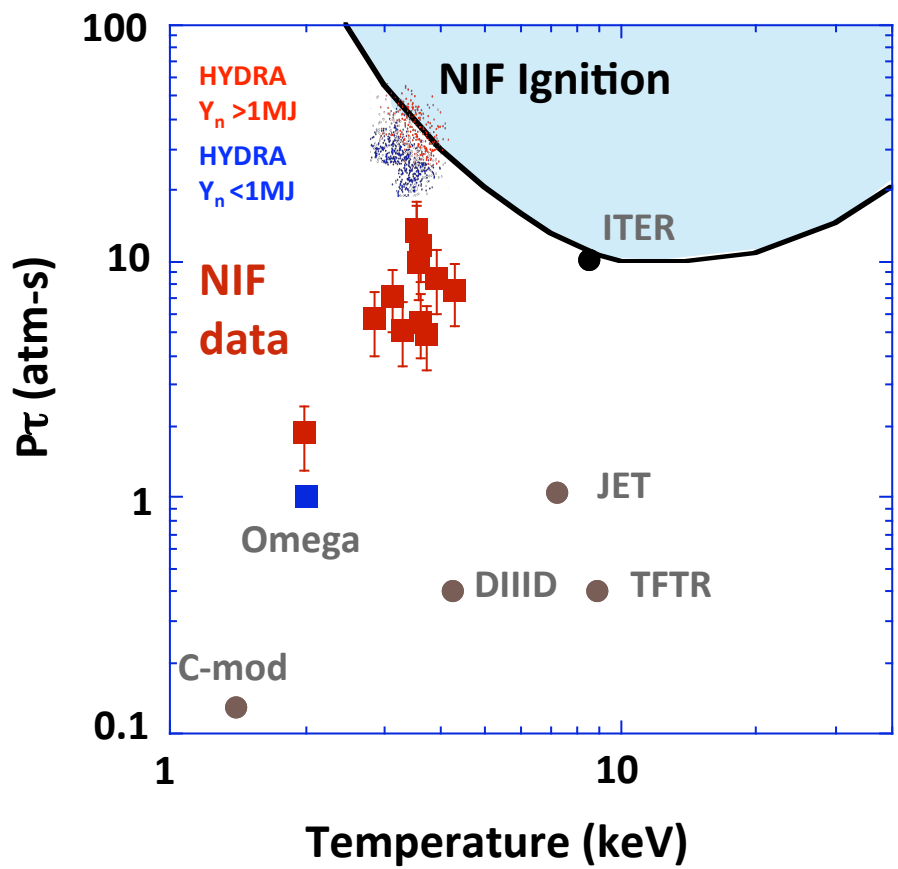

Simulations show > 1MJ yield [ignition] for a factor of 3 higher pressures

Recent papers on NIC

- Symmetry
  - Michel et al., PRL (2009)
  - Glenzer et al., Science (2010)
- Hohlraum Drive
  - Kline et al., PRL (2011)
  - Glenzer et al., PRL (2011)
- Low Entropy and shock timing tuning
  - Mackinnon et al., PRL, in print
  - Robey et al., PRL, in print
  - Doeppner et al., PRL, in print
- Shape tuning
  - Moody et al. Nature Physics, in print
- Mix
  - Regan et al., PRL, submitted
- Nuclear fuel implosions
  - Glenzer et al., POP, submitted
  - Glenzer et al. PPCF, submitted
  - Callahan et al. POP, submitted
  - Spears et al. POP, submitted
  - Jones et al. POP, submitted

High areal density

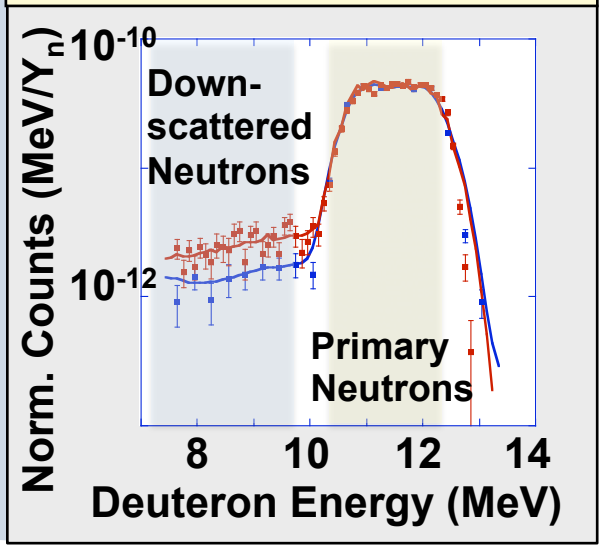

Small hot e$^-$ Preheat

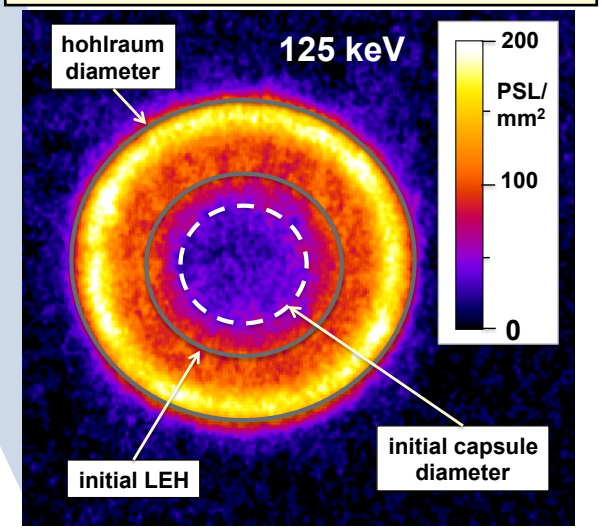

Summary

- We have successfully completed the first integrated ignition tuning experiments by fielding eight $T_{70\text{-}74}H_{20\text{-}24}D_{2\text{-}20}$ and nine $D_{50}T_{50}$ implosions
  - Ability to field cryogenic thermonuclear fuel layers that meet ignition specification
  - Use of varying amounts of deuterium allows for a diagnostic rich environment to measure the assembly of thermonuclear fuel

- These experiments have demonstrated high values for the Lawson fusion confinement criterion
  - Implosion are driven up to 1.6 MJ in >300 eV hohlraums
  - Demonstrated control of implosion shape
  - Demonstrated 8 x 10^{14} DT yield with 10-20% yield over 2-D clean
  - Demonstrated pressures > 100 Gbar and experimental ignition threshold factors of ITFx ~ 0.1

- Optimize final shock (4th rise, Uranium)
- Optimize velocity-mix - trade off

We are at the threshold of delivering a DT platform to measure α−heating

We acquired high quality ablator radiographs from 1st shock break-out (14 ns) to peak velocity (22 ns)

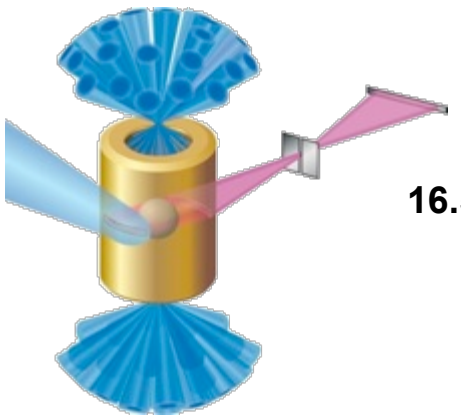

9 keV gated 1D radiographs

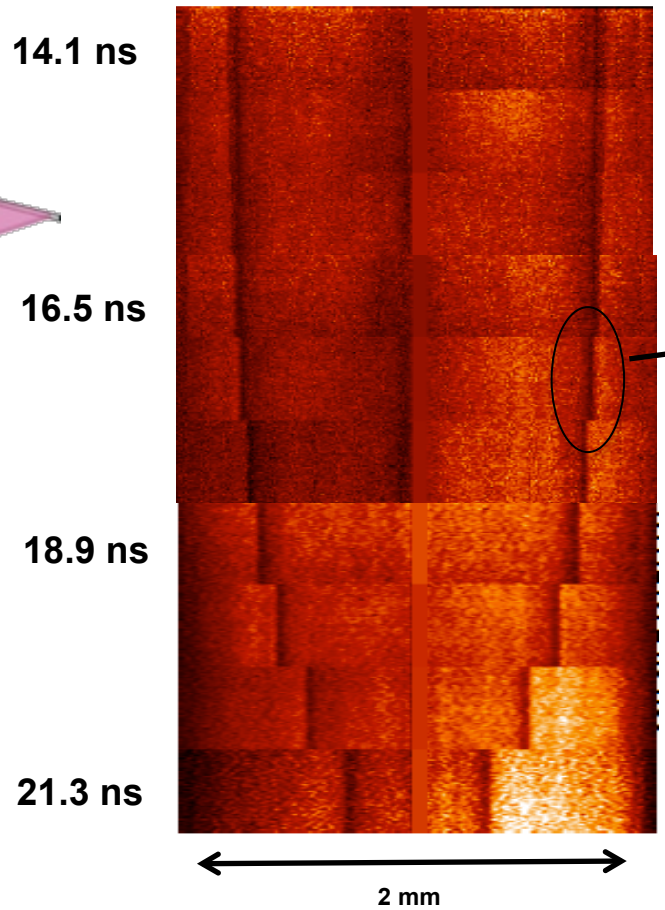

Examples of Transmission lineouts at one limb

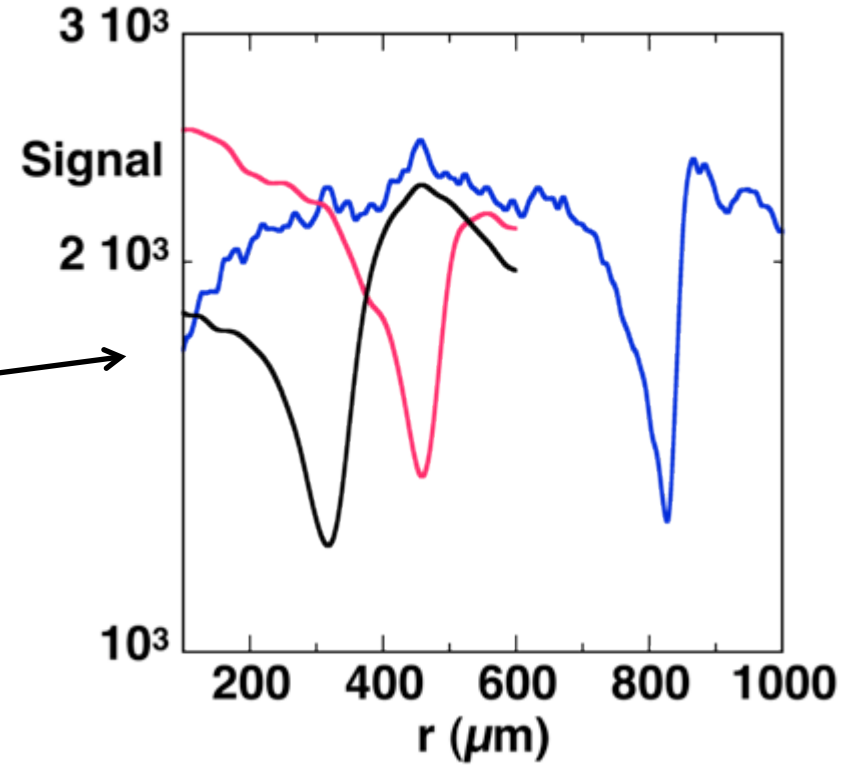

Extract r_{CoM}, v, Δr, mass vs t and ρ vs r for various 4th rise pulse shapes

The Pressure campaign is measuring the effects of three main-pulse rise-rates on implosion conditions

- Black: nominal-rise laser pulse reaches peak power 2 ns after 3rd shock plateau
  - We've been shooting this pulse since April 2011

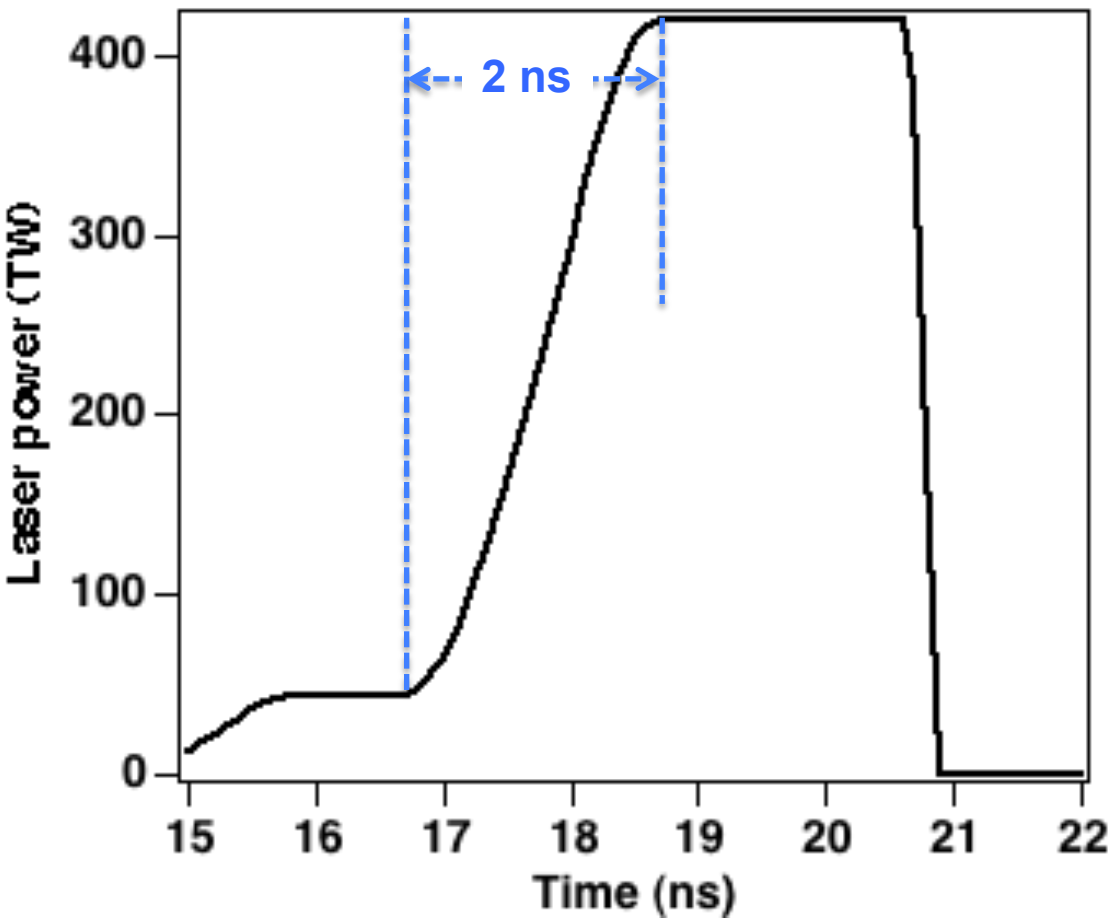

The Pressure campaign is measuring the effects of three main-pulse rise-rates on implosion conditions

- Black: nominal-rise laser pulse reaches peak power 2 ns after 3rd shock plateau
  - We've been shooting this pulse since April 2011
- Blue: slow-rise pulse reaches peak power 3 ns after 3rd shock
  - Gradually ramp up ablation pressure
  - Smooth acceleration may improve fuel or hot-spot ρR

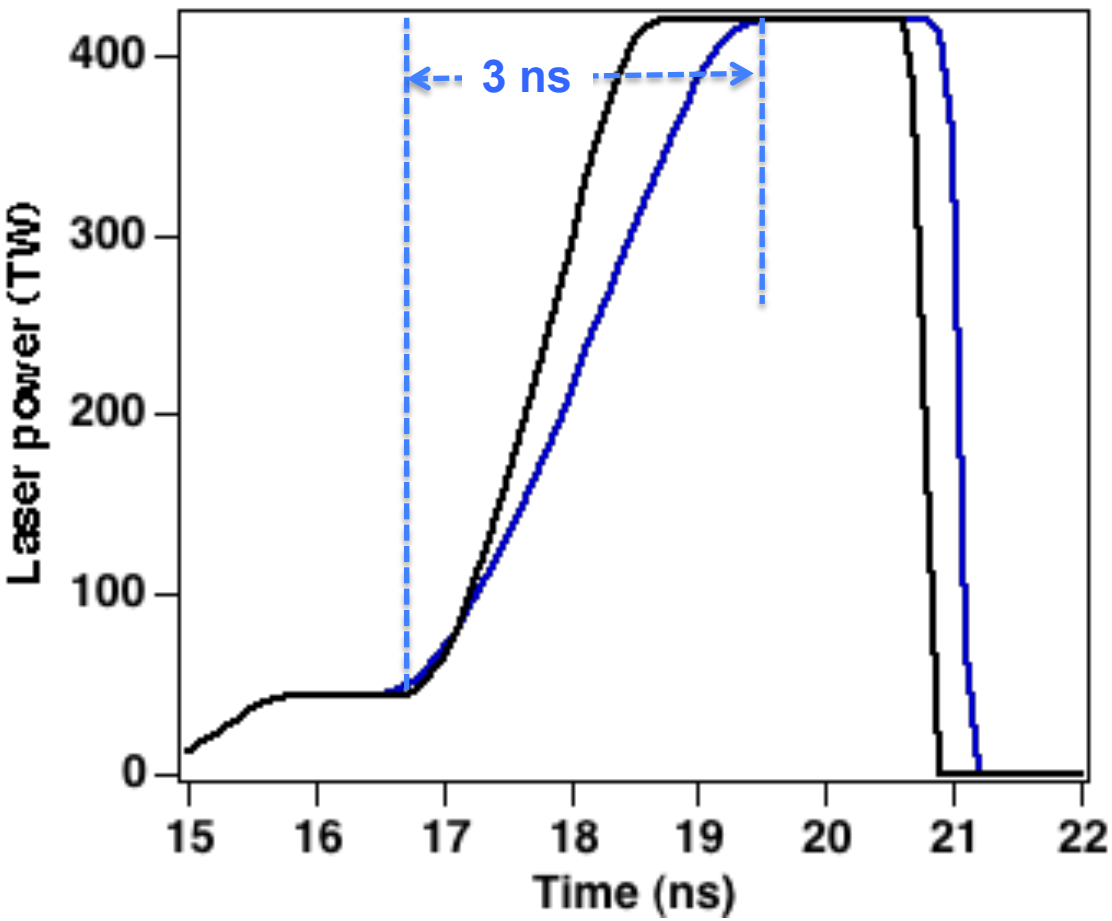

The Pressure campaign is measuring the effects of three main-pulse rise-rates on implosion conditions

- Black: nominal-rise laser pulse reaches peak power 2 ns after 3rd shock plateau
  - We've been shooting this pulse since April 2011
- Blue: slow-rise pulse reaches peak power 3 ns after 3rd shock
  - Gradually ramp up ablation pressure
  - Smooth acceleration may improve fuel or hot-spot ρR
- Red: fast-rise pulse reaches peak power 1 ns after 3rd shock
  - Push capsule hard right as shocks 1-3 break out
  - Maximize absorbed energy

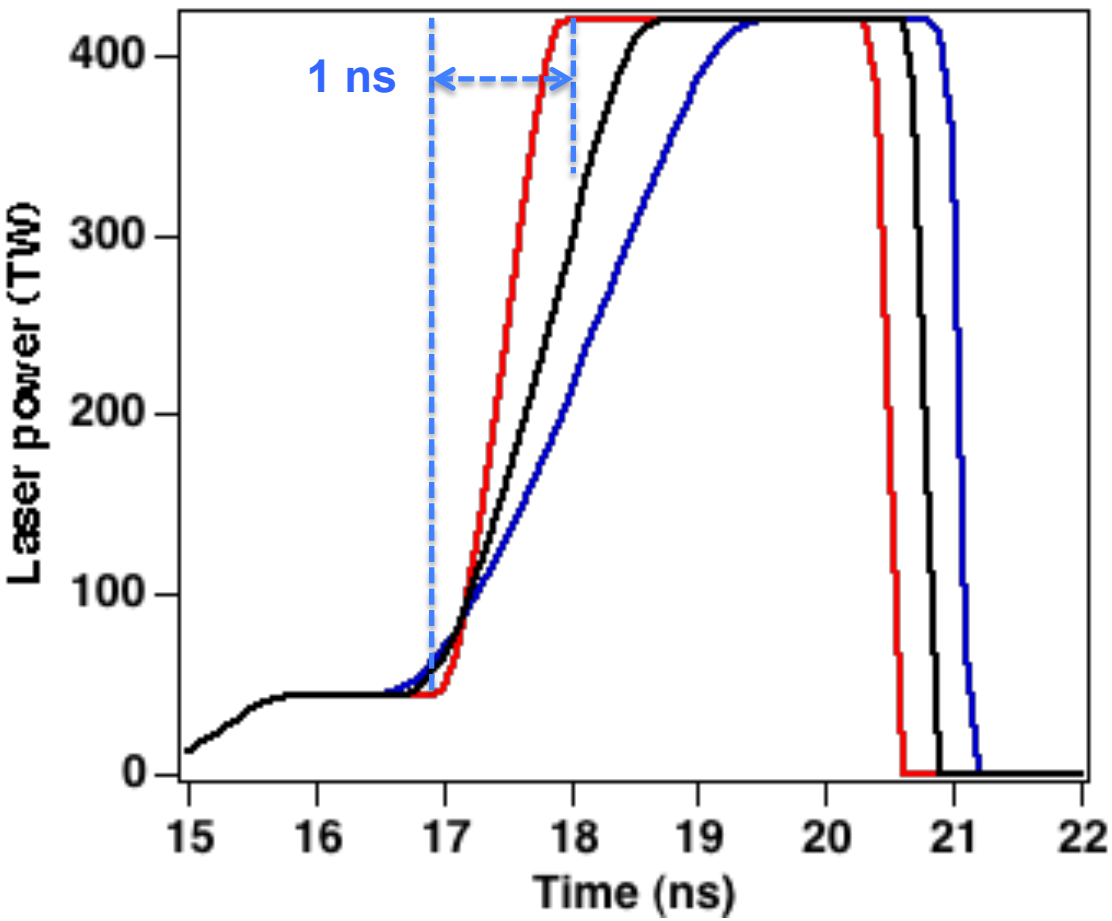

Slowing down the 4th-rise decreases the 4th shock strength and reduces the capsule absorbed energy

Measured leading shock velocity

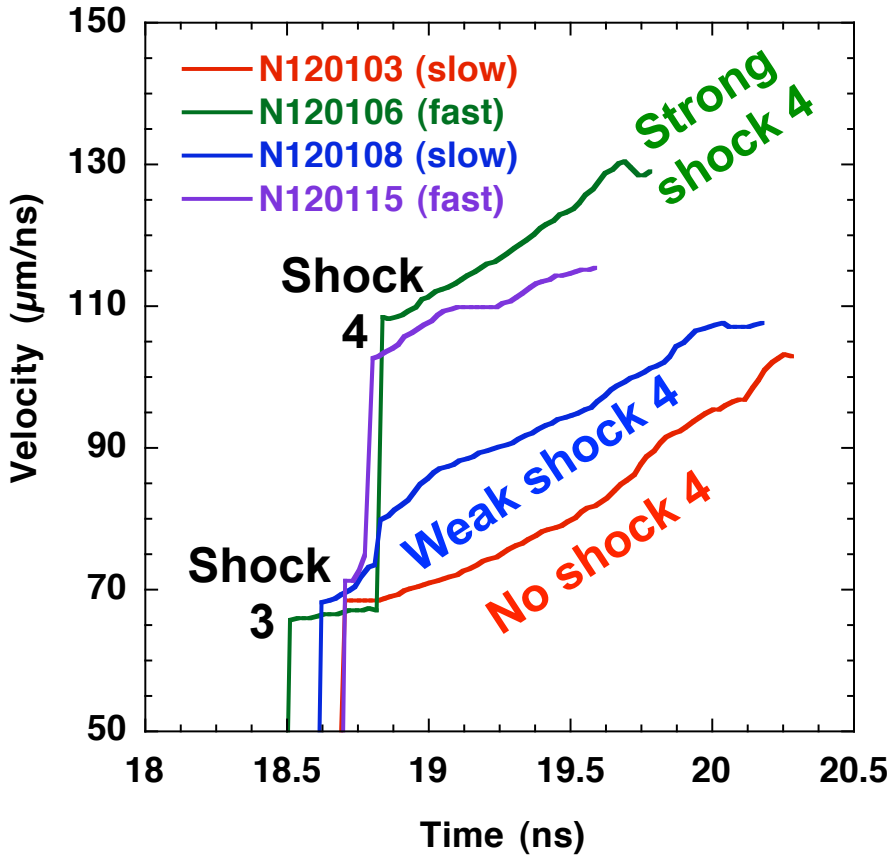

HYDRA absorption rate $R_{abl}^2 \times \sigma T_R^4$

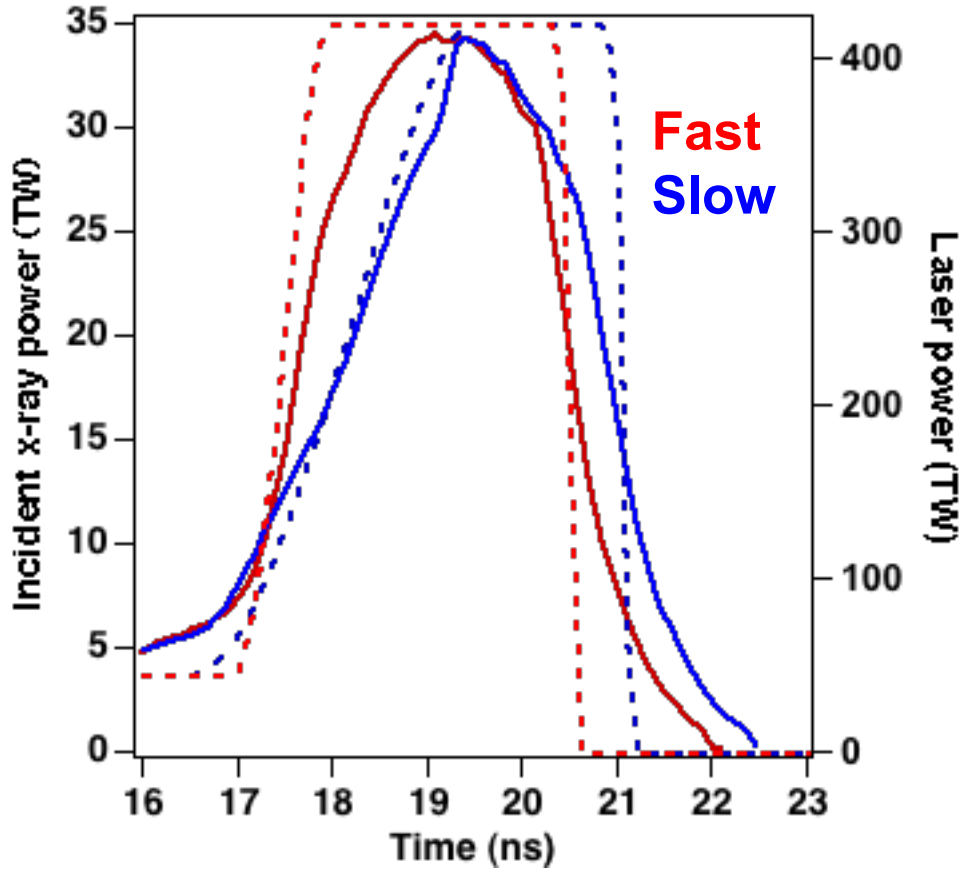

- Slow-rise pulse does not coalesce into a sharp 4th shock
- Fast-rise pulse results in a fast 4th shock

- Fast-rise pulse absorbs energy earlier, at larger radius
- Slow rise absorbs drive gradually

The fast-rise 4th pulse may lead to a thicker ablator than the slow-rise 4th pulse at peak velocity

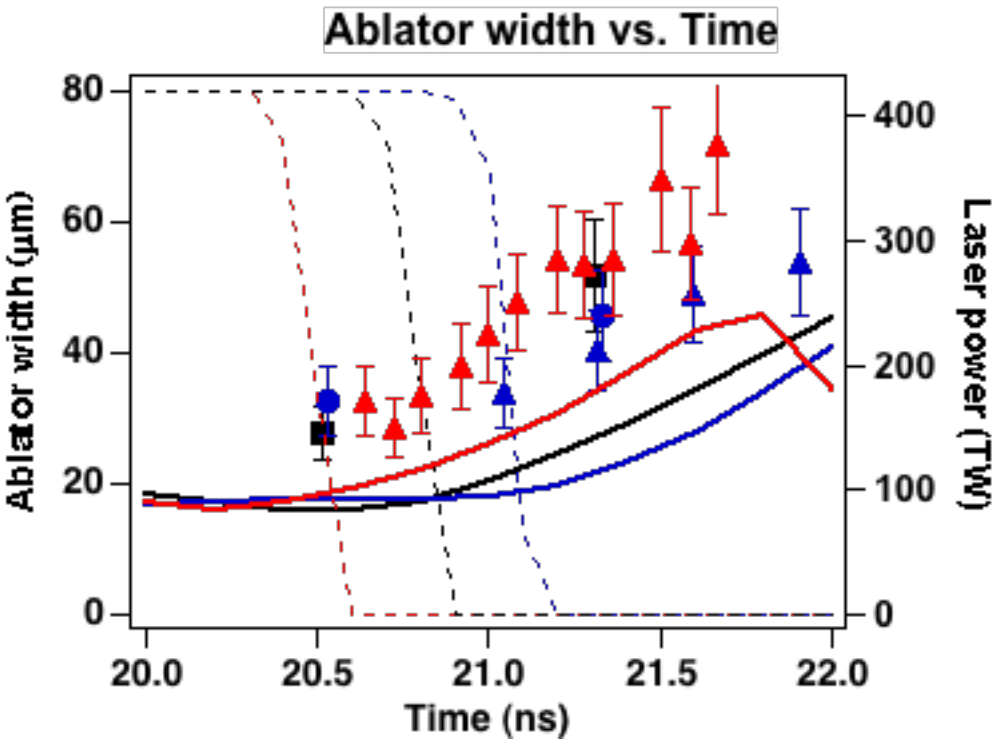

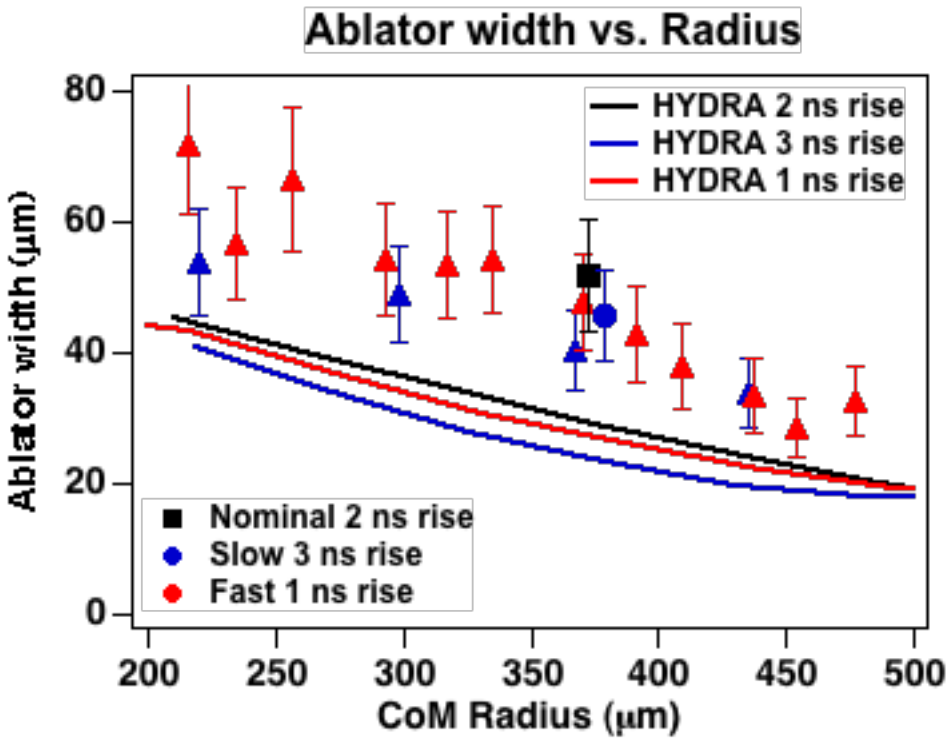

- Difference is comparable to error-bars
- Further analysis is warranted

Most recent DT implosion experiments show efficient compression and a symmetric hot spot

9 keV x-ray emission in the equatorial direction N120205

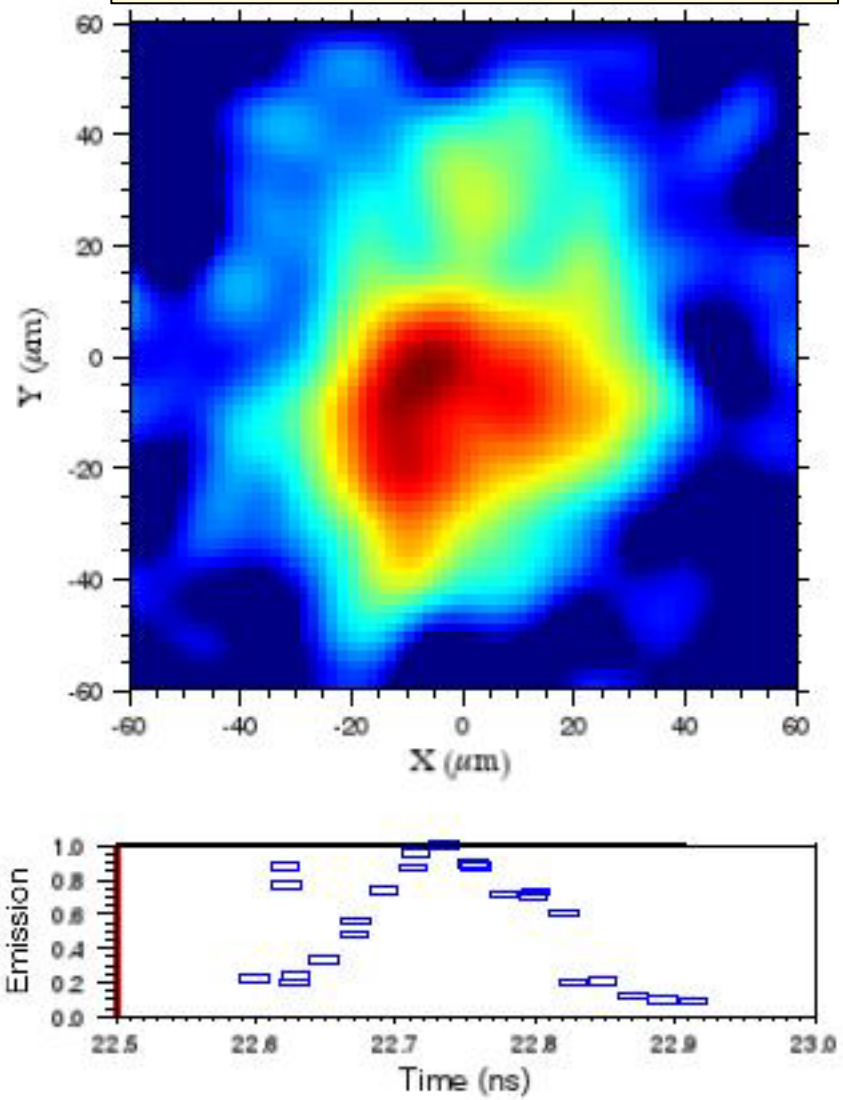

9 keV x-ray emission in the polar direction N120205

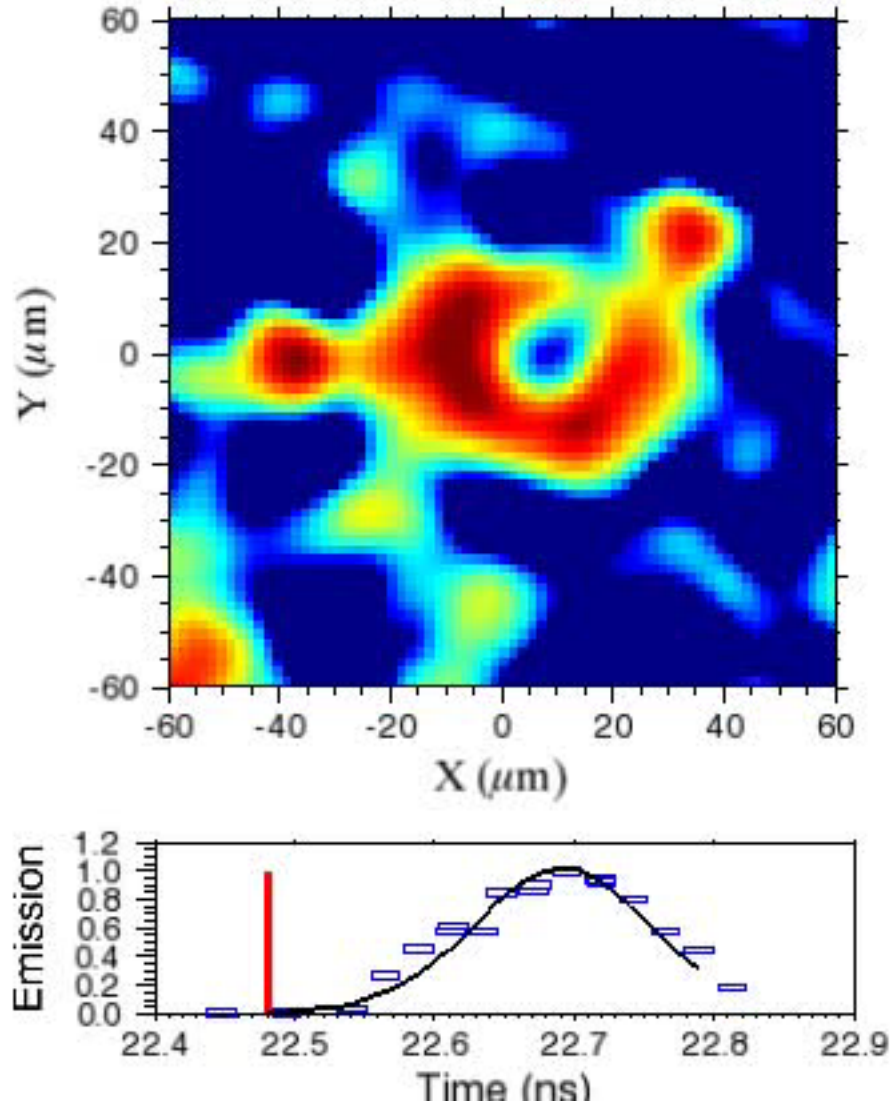

Thanks to the NIF team

M. J. Edwards,1 B. J. MacGowan,1 B. K. Spears,1 P. A. Adams,1 J. B. Alfonso,1 E. T. Alger,1 Z. Alherz,1 L. F. Alvarez,1 S. S. Alvarez,1 P. V. Amick,1 K. S. Andersson,1 S. D. Andrews,1 G. J. Antonini,1 P. A. Arnold,1 D. P. Atkinson,1 L. Auyang,1 S. G. Azevedo,1 B. N. M. Balaoing,1 J. A. Baltz,1 F. Barbosa,1 G. W. Bardsley,1 D. A. Barker,1 A. I. Barnes,1 A. Baron,1 R. G. Beeler,1 B. V. Beeman,1 L. R. Belk,1 J. C. Bell,1 P. M. Bell,1 R. L. Berger,1 M. A. Bergonia,1 L. J. Bernardez,1 L. V. Berzins,1 R. C. Bettenhausen,1 L. Bezerides,1 D. L Bleuel,1 S. D. Bhandarkar,1 C. L. Bishop,1 E. J. Bond,1 D. R. Bopp,1 J. A. Borgman,1 J. R. Bower,1 G. A. Bowers,1 M. W. Bowers,1 D. T. Boyle,1 D. K. Bradley,1 J. L. Bragg,1 J. Braucht,1 D. L. Brinkerhoff,1 D. F. Browning,1 G. K. Brunton,1 S. C. Burkhart,1 S. R. Burns,1 K. E. Burns,1 B. Burr,1 L. M. Burrows,1 R. K. Butlin,1 J. A. Caggiano,1 N. J. Cahayag,1 D. A. Callahan,1 P. S. Cardinale,1 R. W. Carey,1 J. W. Carlson,1 A. D. Casey,1 C. Castro,1 J. R. Celeste,1 C. J. Cerjan,1 G. W. Collins,1 A. Y. Chakicherla,1 F. W. Chambers,1 C. Chan,1 H. Chandrasekaran,1 C. Chang,1 R. F. Chapman,1 K. Charron,1 Y. Chen,1 M. J. Christensen,1 A. J. Churby,1 T. J. Clancy,1 D. S. Clark,1 B. D. Cline,1 L. C. Clowdus,1 D. G. Cocherell,1 F. E. Coffield,1 S. J. Cohen,1 R. L. Costa,1 J. R. Cox,1 G. M. Curnow,1 M. J. Dailey,1 P. M. Danforth,1 R. Darbee,1 P. S. Datte,1 J. A. Davis,1 G. A. Deis,1 R. D. Demaret,1 E. L. Dewald,1 P. Di Nicola,1 J. M. Di Nicola,1 L. Divol,1 S. Dixit,1 D. B. Dobson,1 T. Doppner,1 J. D. Driscoll,1 J. Dugorepec,1 J. J. Duncan,1 P. C. Dupuy,1 R. Dylla-Spears,1 E. G. Dzenitis,1 M. J. Eckart,1 S. L. Edson,1 G. J. Edwards,1 O. D. Edwards,1 P. W. Edwards,1 J. C. Ellefson,1 C. H. Ellerbee,1 G. V. Erbert,1 C. M. Estes,1 W. J. Fabyan,1 J. E. Fair,1 R. N. Fallejo,1 M. Fedorov,1 B. Felker,1 J. T Fink,1 M. D. Finney,1 L. F. Finnie,1 M. J. Fischer,1 J. M. Fisher,1 B. T. Fishler,1 J. W. Florio,1 A. Forsman,1 C. B. Foxworthy,1 R. M. Franks,1 T. Frazier,1 G. Frieder,1 T. Fung,1 G. N. Gawinski,1 C. R. Gibson,1 E. Giraldez,1 S. M. Glenn,1 B. P. Golick,1 H. Gonzales,1 S. A. Gonzales,1 M. J. Gonzalez,1 K. L. Griffin,1 J. Grippen,1 S. M. Gross,1 P. H. Gschweng,1 G. Gururangan,1 K. Gu,1 S. W. Haan,1 S. R. Hahn,1 B. J. Haid,1 J. E. Hamblen,1 B. A. Hammel,1 A. V. Hamza,1 D. L. Hardy,1 D. R. Hart,1 R. G. Hartley,1 C. A. Haynam,1 G. M. Heestand,1 M. R. Hermann,1 G. L. Hermes,1 D. S. Hey,1 R. L. Hibbard,1 D. G. Hicks,1 D. E. Hinkel,1 D. L. Hipple,1 J. D. Hitchcock,1 D. L. Hodtwalker,1 J. P. Holder,1 J. D. Hollis,1 G. M. Holtmeier,1 D. M. Holunga,1 J. B. Horner,1 H. Huang,1 S. R. Huber,1 A. W. Huey,1 D. N. Hulsey,1 S. L. Hunter,1 T. R. Huppler,1 M. S. Hutton,1 N. Izumi,1 J. L. Jackson,1 M. A. Jackson,1 K. S. Jancaitis,1 D. R. Jedlovec,1 B. Johnson,1 M. C. Johnson,1 T. Johnson,1 M. P. Johnston,1 O. S. Jones,1 D. H. Kalantar,1 J. H. Kamperschroer,1 R. L. Kauffman,1 G. A. Keating,1 L. M. Kegelmeyer,1 S. L. Kenitzer,1 J. R. Kimbrough,1 K. King,1 R. K. Kirkwood,1 J. L. Klingmann,1 K. M. Knittel,1 T. R. Kohut,1 K. G. Koka,1 B. Kozioziemski,1 S. W. Kramer,1 J. E. Krammen,1 K. G. Krauter,1 G. W. Krauter,1 E. K. Krieger,1 A. L. Kritcher,1 J. J. Kroll,1 K. N. La Fortune,1 L. J. Lagin,1 V. K. Lakamsani,1 O. L. Landen,1 S. W. Lane,1 A. B. Langdon,1 S. H. Langer,1 N. Lao,1 D. W. Larson,1 D. Latray,1 G. T. Lau,1 S. Le Pape,1 B. L. Lechleiter,1 Y. Lee,1 T. L. Lee,1 J. Li,1 J. A. Liebman,1 J. D. Lindl,1 S. F. Locke,1 H. K. Loey,1 R. A. London,1 F. J. Lopez,1 D. M. Lord,1 R. R. Lowe-Webb,1 J. G. Lown,1 A. P. Ludwigsen,1 N. W. Lum,1 R. R. Lyons,1 T. Ma,1 A. J. MacKinnon,1 M. D. Magat,1 D. T. Maloy,1 T. N. Malsbury,1 E. Mapoles,1 G. Markham,1 R. M. Marquez,1 A. A. Marsh,1 C. D. Marshall,1 S. R. Marshall,1 I. L. Maslennikov,1 D. G. Mathisen,1 G. J. Mauger,1 M. -Y. Mauvais,1 J. A. McBride,1 T. McCarville,1 J. B. McCloud,1 A. McGrew,1 B. McHale,1 A. G. MacPhee,1 J. F. Meeker,1 N. B. Meezan,1 J. S. Merill,1 E. P. Mertens,1 P. A. Michel,1 M. G. Miller,1 T. Mills,1 J. L. Milovich,1 R. Miramontes,1 R. C. Montesanti,1 M. M. Montoya,1 J. Moody,1 J. D. Moody,1 M. Moran,1 K. A. Moreno,1 J. Morris,1 K. M. Morriston,1 D H Munro,1 B. R. Nathan,1 J. R. Nelson,1 M. Neto,1 J. D. Neumann,1 E. Ng,1 Q. M. Ngo,1 B. L. Olejniczak,1 C. D. Orth,1 N. L. Orsi,1 M. W. Owens,1 E. H. Padilla,1 T. M. Pannell,1 T. G. Parham,1 R. W. Patterson, Jr.,1 A. Pak,1 P. K. Patel,1 G. Pavel,1 R. R. Prasad,1 D. Pendlton,1 F. A. Penko,1 B. L. Pepmeier,1 D. E. Petersen,1 T. W. Phillips,1 D. Pigg,1 K. W. Piston,1 K. D. Pletcher,1 C. L. Powell,1 H. B. Radousky,1 B. S. Raimondi,1 J. E. Ralph,1 R. L. Rampke,1 R. K. Reed,1 W. A. Reid,1 V. V. Rekow,1 J. L. Reynolds,1 J. J. Rhodes,1 M. J. Richardson,1 R. J. Rinnert,1 B. P. Riordan,1 A. S. Rivenes,1 A. T. Rivera,1 C. J. Roberts,1 H. F. Robey,1 J. A. Robinson,1 R. B. Robinson,1 S. R. Robison,1 O. R. Rodriguez,1 S. P. Rogers,1 M. D. Rosen,1 G. F. Ross,1 J. Steven Ross,1 M. Runkel,1 A. S. Runtal,1 R. A. Sacks,1 J. Sater,1 S. F. Sailors,1 J. T. Salmon,1 J. D. Salmonson,1 R. L. Saunders,1 J. R. Schaffer,1 T. M. Schindler,1 M. J. Schmitt,1 M. B. Schneider,1 K. S. Segraves,1 M. J. Shaw,1 M. E. Sheldrick,1 R. T. Shelton,1 M. K. Shiflett,1 S. J. Shiromizu,1 M. Shor,1 L. L. Silva,1 S. A. Silva,1 K. M. Skulina,1 D. A. Smauley,1 B. E. Smith,1 L. K. Smith,1 A. L. Solomon,1 S. Sommer,1 J. G. Soto,1 N. I. Spafford,1 D. E. Speck,1 P. T. Springer,1 M. Stadermann,1 F. Stanley,1 T. G. Stone,1 E. A. Stout,1 P. L. Stratton,1 R. J. Strausser,1 L. J. Suter,1 W. Stoeffl,1 W. Sweet,1 M. F. Swisher,1 J. D. Tappero,1 J. B. Tassano,1 J. S. Taylor,1 E. A. Tekle,1 C. Thai,1 C. A. Thomas,1 A. Thomas,1 A. L. Throop,1 G. L. Tietbohl,1 J. M. Tillman,1 R. P. J. Town, 1 S. L. Townsend,1 K. L. Tribbey,1 D. Trummer,1 J. Truong,1 J. Vaher,1 M. Valadez,1 P. Van Arsdall,1 A. J. Van Prooyen,1 E. O. Vergel de Dios,1 M. D. Vergino,1 S. P. Vernon,1 J. L. Vickers,1 G. T. Villanueva,1 M. A. Vitalich,1 S. A. Vonhof,1 F. E. Wade,1 R. J. Wallace,1 C. T. Warren,1 A. L. Warrick,1 C. Walters,1 J. Watkins,1 S. Weaver, 1 P. J. Wegner,1 M. A. Weingart,1 J. Wen,1 K. S. White,1 P. K. Whitman,1 K. Widmann,1 C. C. Widmayer,1 K. Wilhelmsen,1 E. A. Williams,1 W. H. Williams,1 L. Willis,1 E F. Wilson,1 B. A. Wilson,1 M. C. Witte,1 K. Work,1 P. S. Yang,1 B. K. Young,1 K. P. Youngblood,1 R. A. Zacharias,1 T. Zaleski,1 P. G. Zapata,1 H. Zhang,1 J. S. Zielinski,1 J. L. Kline,2 G. A. Kyrala,2 H. W. Herrmann,2 D. C. Wilson,2 R. C. Leepr,3 R. E. Olson,3 J. D. Kilkenny,4 A. Nikroo,4 C. Niemann,5 V. Glebov,6 James P. Knauer,6 S. P. Regan,6 T. C. Sangster,6 L. J. A. Frenje,7 M. Gatu Johnson,7 R. Petrasso,7 H. Rinderknecht,7 A.Zylstra,7 A. S Moore,8 B. M. Van Wonterghem,1 L. J. Atherton,1 and E. I. Moses1

1 Lawrence Livermore National Laboratory, Livermore, California 94550, USA, 2 Los Alamos National Laboratory, Los Alamos, New Mexico 87545, USA,
3 Sandia National Laboratory, Sandia, New Mexico 87185, USA, 4 General Atomics, San Diego, California 92121 , USA, 5 University of California Los Angeles, CA, USA
6 Laboratory for Laser Energetics, University of Rochester, Rochester, New York 14623, USA, 7 Plasma Fusion and Science Center, Massachusetts Institute of Science and Technology, Cambridge, Massachusetts 02139, USA, 8 Atomic Weapons Establishment, Aldermaston, RG7, UK

We have prepared a high-velocity DU implosion platform to provide margin for mix and to reach the alpha-heating regime

Selected actionable parameters

Laser campaign
Energy/Power

- 450 TW, 1.6 MJ
- 420 TW, 1.8 MJ
- Energy reproducibility, 5% foot, 3% peak adj. thres. (✓)

Shape campaign
Hohlraum Drive

- DU ✓
- 3.1 mm LEH, DU pointing ✓
- $\Delta\lambda_2$ = 6.6 Å, $\Delta\lambda_3$ = 8.1 Å (✓)

Pressure campaign
Pulse Shape

- Slow 4th rise
- Fast 4th rise
- DU shock timing [closed 2nd, 3rd gap]

Mix campaign
Capsule

- Nominal ablator 2% Si
- Nominal ablator 4% Si
- Thick ablator 2% Si
- Thick ablator 4% Si

DU equator view
P_2/P_0= 5.6%
P_0 = 49 ± 1 μm

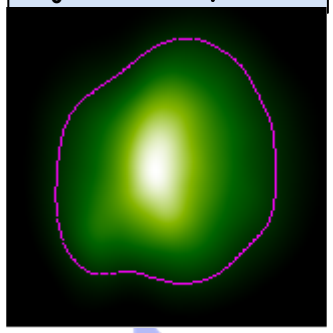

DU polar view
M_4/M_0= 3.3%
P_0 = 65 ± 1 μm

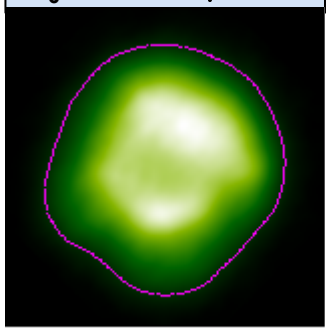

April 2012

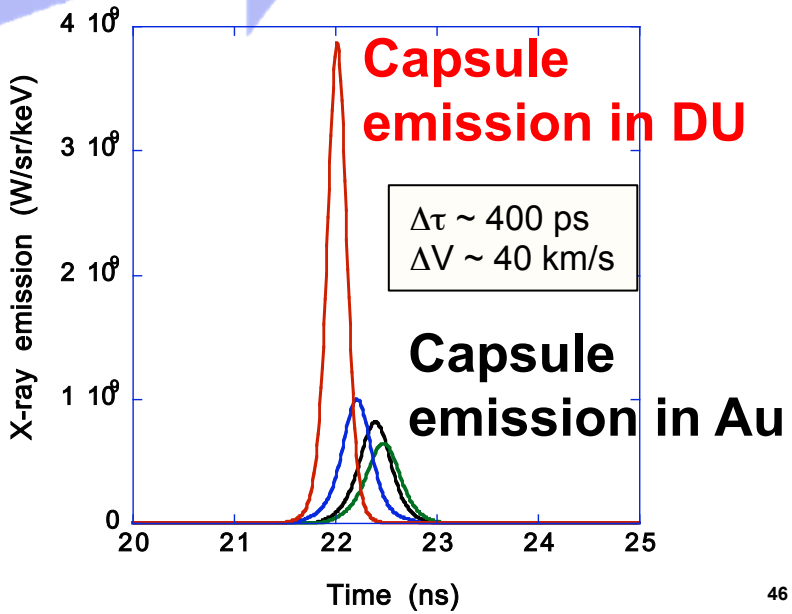

NIC